

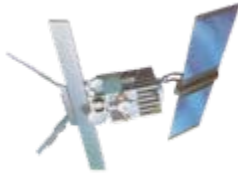
# Optimal Spectral Decomposition (OSD) for Analyzing Sparse and Noisy Ocean Data

Sponsors: NOAA/NODC, ONR, NAVO

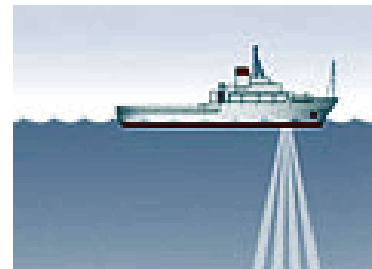
Peter C Chu  
Naval Postgraduate School  
Monterey, CA 93943

[pcchu@nps.edu](mailto:pcchu@nps.edu)

<http://faculty.nps.edu/pcchu>



# How can we effectively use observational ocean data to represent and to predict the ocean state?



# Collaborators

- Charles Sun (NOAA/NODC)
- Leonid M. Ivanov (California State Univ)
- Chenwu Fan (NPS)
- Tateana Margolina (NPS)
- Oleg Melnichenko (Univ of Hawaii)

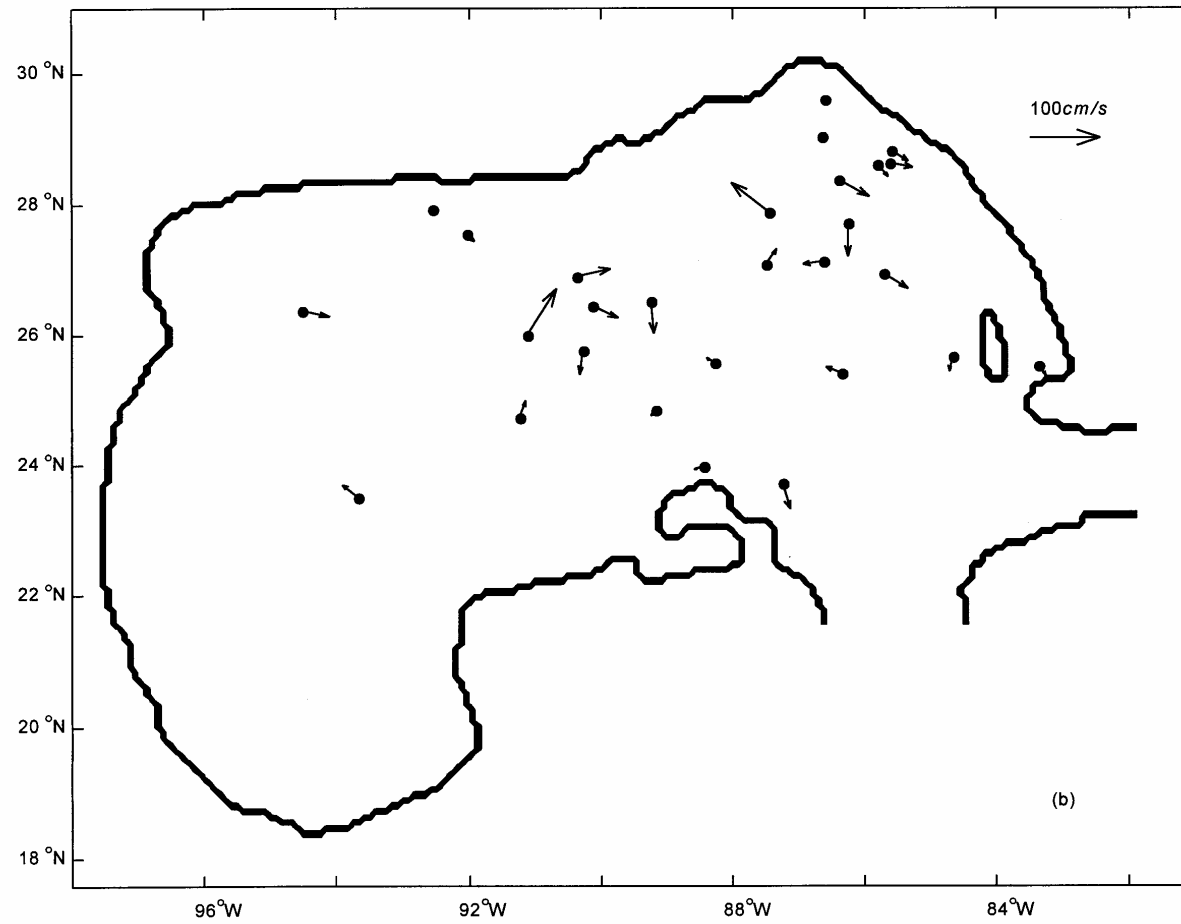
# References

- Chu, P.C., L.M. Ivanov, T.P. Korzhova, T.M. Margolina, and O.M. Melnichenko, 2003a: Analysis of sparse and noisy ocean current data using flow decomposition. Part 1: Theory. *Journal of Atmospheric and Oceanic Technology*, 20 (4), 478-491.
- Chu, P.C., L.M. Ivanov, T.P. Korzhova, T.M. Margolina, and O.M. Melnichenko, 2003b: Analysis of sparse and noisy ocean current data using flow decomposition. Part 2: Application to Eulerian and Lagrangian data. *Journal of Atmospheric and Oceanic Technology*, 20 (4), 492-512.
- Chu, P.C., L.M. Ivanov, and T.M. Margolina, 2004: Rotation method for reconstructing process and field from imperfect data. *International Journal of Bifurcation and Chaos*, 14 (04), 2991-2997.

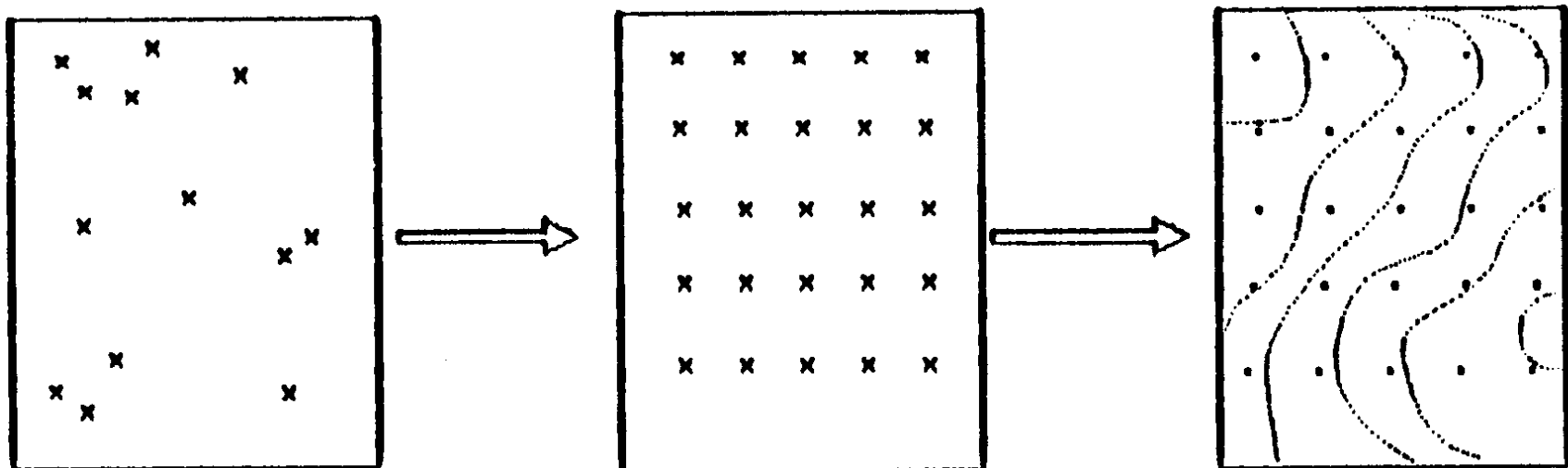
# References

- Chu, P.C., L.M. Ivanov, and T.M. Margolina, 2005: Seasonal variability of the Black Sea Chlorophyll-a concentration. *Journal of Marine Systems*, 56, 243-261.
- Chu, P.C., L.M. Ivanov, and O.M. Melnichenko, 2005: Fall-winter current reversals on the Texas-Louisiana continental shelf. *Journal of Physical Oceanography*, 35, 902-910.
- Chu, P.C., L.M. Ivanov, O.V. Melnichenko, and N.C. Wells, 2007: On long baroclinic Rossby waves in the tropical North Atlantic observed from profiling floats. *Journal of Geophysical Research*, 112, C05032, doi:10.1029/2006JC003698.
- Chu, P.C., L.M. Ivanov, O.V. Melnichenko, and N.C. Wells, 2007: On long baroclinic Rossby waves in the tropical North Atlantic observed from profiling floats. *Journal of Geophysical Research*, 112, C05032, doi:10.1029/2006JC003698 .

# Observational Data (Sparse and Noisy)



# A Popular Method for Ocean Data Analysis: Optimum Interpolation (OI)



# OI – Equation

Grid point  $\rightarrow k$ , Observational Point  $\rightarrow j$

$Q_k^f \rightarrow$  First guess field (gridded)

$Q_j^o \rightarrow$  Observation

$Q_j^f \rightarrow$  First guess interpolated on the observational point

$$Q_k^a = Q_k^f + \sum_{j=1}^N \alpha_{kj} (Q_j^o - Q_j^f)$$

$Q_k^a \rightarrow$  Analyzed field at the grid point

# OI – Weight Coefficients $\alpha_{kj}$

$$\sum_{j=1}^N (\eta_{ij} + \delta_{ij} \lambda_i^o) \alpha_{kj} = \eta_{kj}$$

$\eta_{ij}$        $\eta_{kj}$       → Autocorrelation functions

$\lambda_i^o$       → Signal-to-noise ratio

# Three Requirements for the OI Method

- (1) First guess field
- (2) Autocorrelation functions
- (3) High signal-to-noise ratio

# Ocean Velocity Data

- (1) First guess field (?)
- (2) Unknown autocorrelation function
- (3) Low signal-to-noise ratio

It is not likely to use the OI  
method to process ocean velocity  
data.

# Spectral Representation - a Possible Alternative Method

$$c(\mathbf{x}, z_k, t) = A_0(z_k, t) + \sum_{m=1}^M A_m(z_k, t) \Psi_m(\mathbf{x}, z_k),$$

$\Psi_m \rightarrow$  Basis functions

# Spectral Representation for Velocity

# Flow Decomposition

- 2 D Flow (Helmholtz)

$$\mathbf{u}_H = \mathbf{r} \times \nabla_H A_1 + \nabla_H A_3$$

- 3D Flow (Toroidal & Poloidal): Very popular in astrophysics

- 

$$\mathbf{u} = \mathbf{r} \times \nabla A_1 + \mathbf{r} A_2 + \nabla A_3$$

# 3D Incompressible Flow

- When

$$\nabla \cdot \mathbf{u} = 0$$

- We have

$$\mathbf{u} = \nabla \times (\mathbf{r}\Psi) + \nabla \times \nabla \times (\mathbf{r}\Phi).$$

# Flow Decomposition

$$u = \frac{\partial \Psi}{\partial y} + \frac{\partial^2 \Phi}{\partial x \partial z}, \quad v = -\frac{\partial \Psi}{\partial x} + \frac{\partial^2 \Phi}{\partial y \partial z},$$

- 

$$\Delta \Psi = -\zeta$$

$$\Delta \Phi = -w$$

# Basis Functions (Closed Basin)

$$\Delta \Psi_k = -\lambda_k \Psi_k, \quad \Psi_k|_{\Gamma} = 0, \quad k = 1, \dots, \infty$$

$$\Delta \Phi_m = -\mu_m \Phi_m, \quad \frac{\partial \Phi_m}{\partial n}|_{\Gamma} = 0, \quad m = 1, \dots, \infty.$$

# Basis Functions (Open Boundaries)

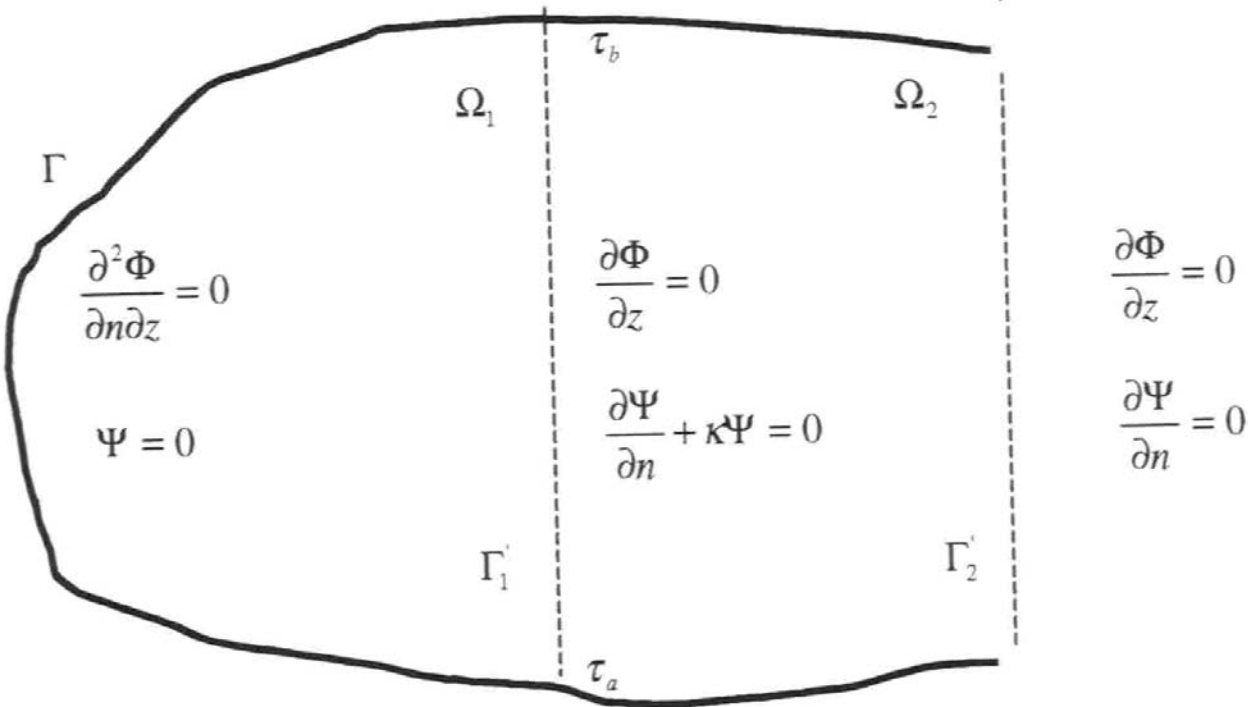
$$\Delta \Psi_k = -\lambda_k \Psi_k,$$

$$\Delta \Phi_m = -\mu_m \Phi_m,$$

$$\Psi_k|_{\Gamma} = 0, \quad \frac{\partial \Phi_m}{\partial n}|_{\Gamma} = 0,$$

$$\left[ \frac{\partial \Psi_k}{\partial n} + \kappa(\tau) \Psi_k \right] |_{\Gamma'_1} = 0, \quad \Phi_m|_{\Gamma'_1} = 0,$$

# Boundary Conditions



# Spectral Decomposition

$$\begin{aligned} u_{KM} &= \sum_{k=1}^K a_k(z, t^\circ) \frac{\partial \Psi_k(x, y, z, \kappa^\circ)}{\partial y} + \sum_{m=1}^M b_m(z, t^\circ) \frac{\partial \Phi_m(x, y, z)}{\partial x}, \\ v_{KM} &= - \sum_{k=1}^K a_k(z, t^\circ) \frac{\partial \Psi_k(x, y, z, \kappa^\circ)}{\partial x} + \sum_{m=1}^M b_m(z, t^\circ) \frac{\partial \Phi_m(x, y, z)}{\partial y} \end{aligned}$$

# Benefits of Using OSD

- (1) Don't need first guess field
- (2) Don't need autocorrelation functions
- (3) Don't require high signal-to-noise ratio
- (4) Basis functions are pre-determined before the data analysis.

# Optimal Mode Truncation

$$J(a_1, \dots, a_K, b_1, \dots, b_M, \kappa, P) = \frac{1}{2} \left( \|u_p^{obs} - u_{KM}\|_P^2 + \|v_p^{obs} - v_{KM}\|_P^2 \right) \rightarrow \min,$$

# Vapnik (1983) Cost Function

$$J_{emp} = J(a_1, \dots, a_K, b_1, \dots, b_M, \kappa, P).$$

$$\text{Prob} \left\{ \sup_{K,M,S} |\langle J(K, M, S) \rangle - J_{emp}(K, M, S)| \geq \mu \right\} \leq g(P, \mu)$$

$$\lim_{P \rightarrow \infty} g(P, \mu) = 0$$

# Optimal Truncation

- Gulf of Mexico, Monterey Bay, Louisiana-Texas Shelf, North Atlantic
- $K_{opt} = 40$ ,  $M_{opt} = 30$

# Determination of Spectral Coefficients (III- Posed Algebraic Equation)

$$\mathbf{A} \hat{\mathbf{a}} = \mathbf{Q} \mathbf{Y},$$

This is caused by the features of  
the matrix  $\mathbf{A}$ .

# Rotation Method (Chu et al., 2004)

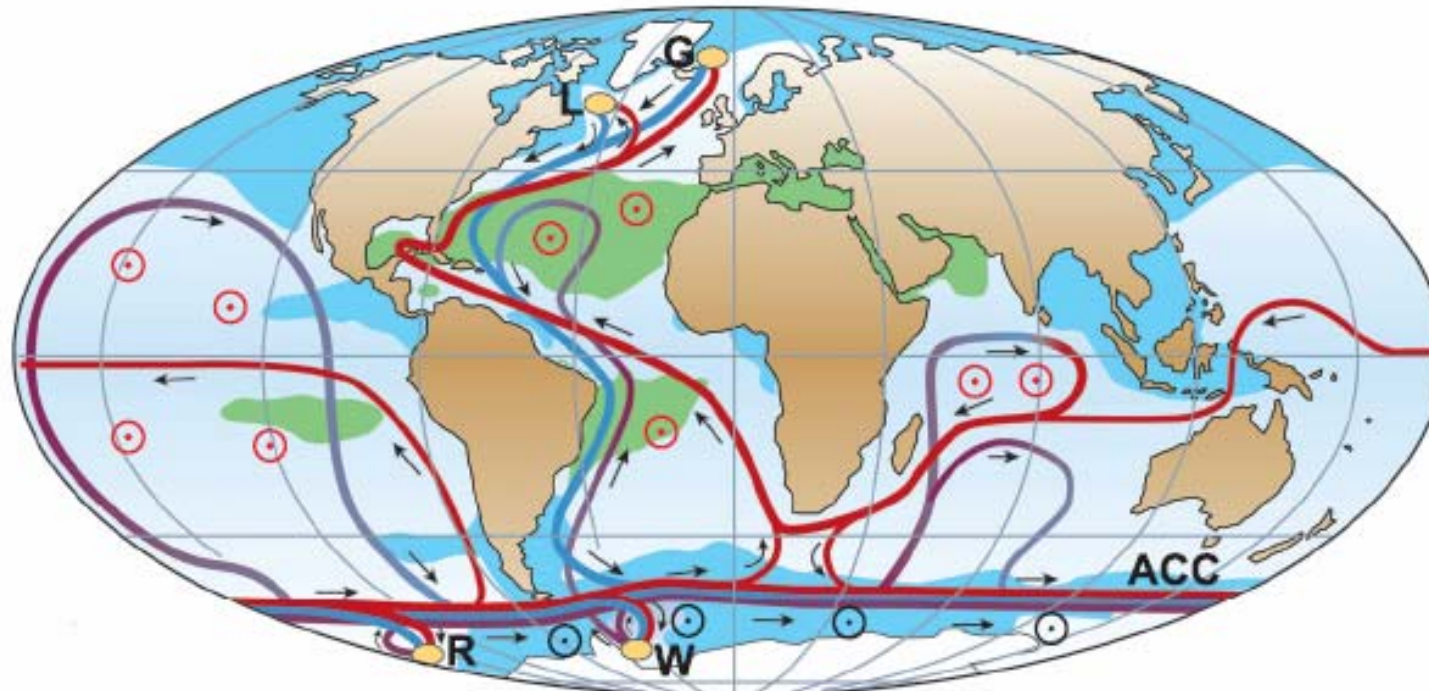
$$\mathbf{S}\mathbf{A}\hat{\mathbf{a}} = \mathbf{SQY},$$

$$J_1 = \|\mathbf{A}\|^2 - \frac{\|\mathbf{SQY}\|^2}{\|\mathbf{a}\|^2} \rightarrow \max,$$

# Example-1 OSD for Analyzing ARGO Data

Baroclinic Rossby Waves in the tropical North Atlantic

# Tropical North Atlantic ( $4^{\circ}$ - $24^{\circ}$ N) Important Transition Zone → Meridional Overturning Circulation (MOC) (Rahmstorf 2006)



— Surface flow  
— Deep flow  
— Bottom flow  
○ Deep Water Formation

○ Wind-driven upwelling  
○ Mixing-driven upwelling  
■ Salinity > 36 ‰  
■ Salinity < 34 ‰

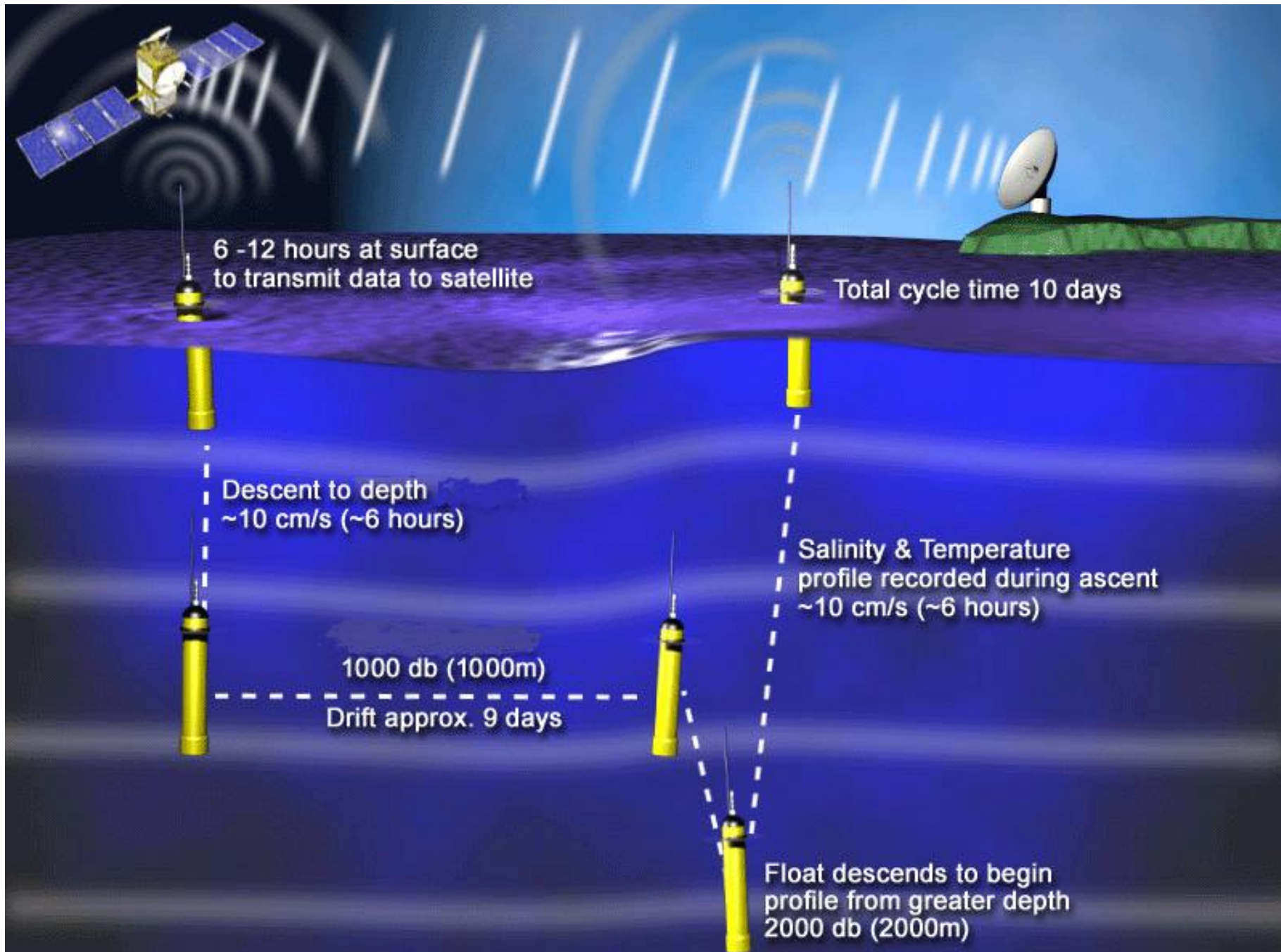
L Labrador Sea  
G Greenland Sea  
W Weddell Sea  
R Ross Sea

MOC Variation →

Heat Transport Variation →

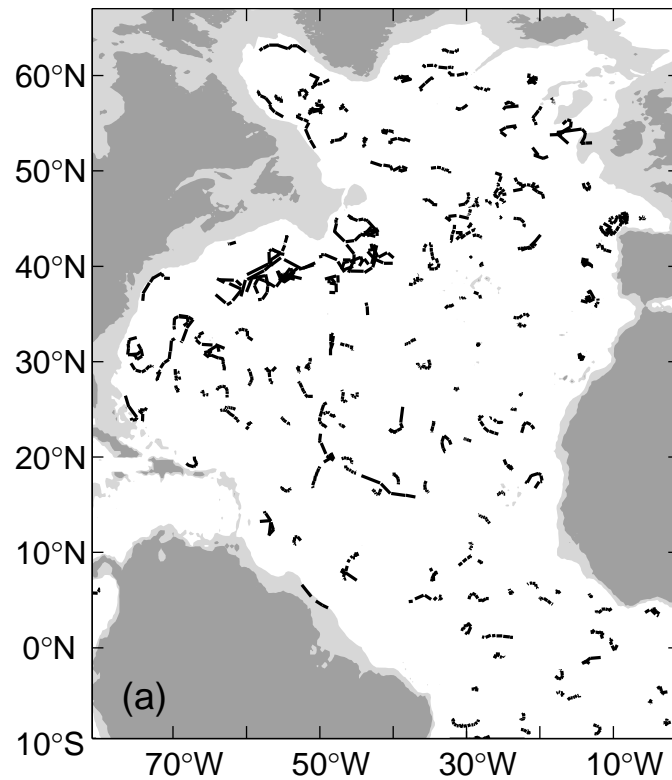
Climate Change

- Are mid-depth (~1000 m) ocean circulations steady?
- If not, what mechanisms cause the change? (Rossby wave propagation)

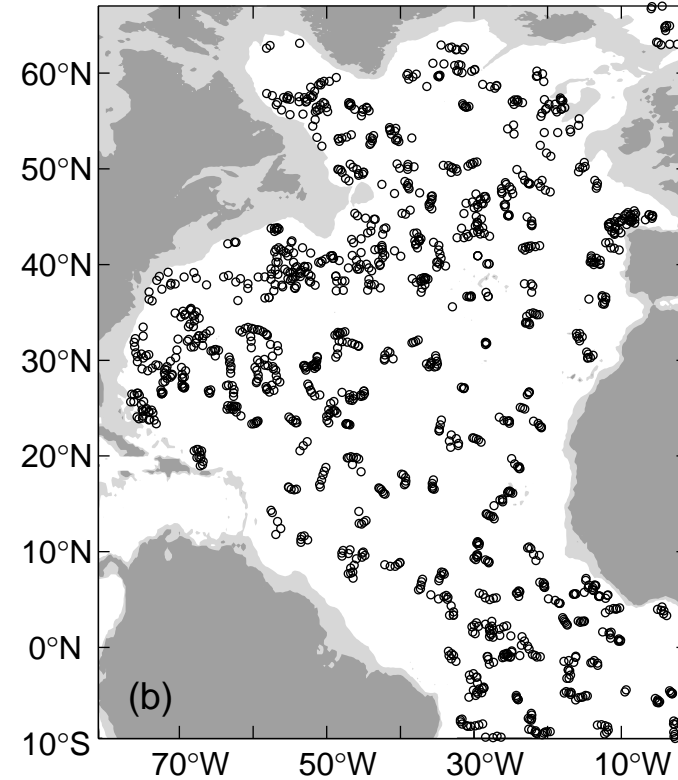


# ARGO Observations (Oct-Nov 2004)

(a) Subsurface tracks

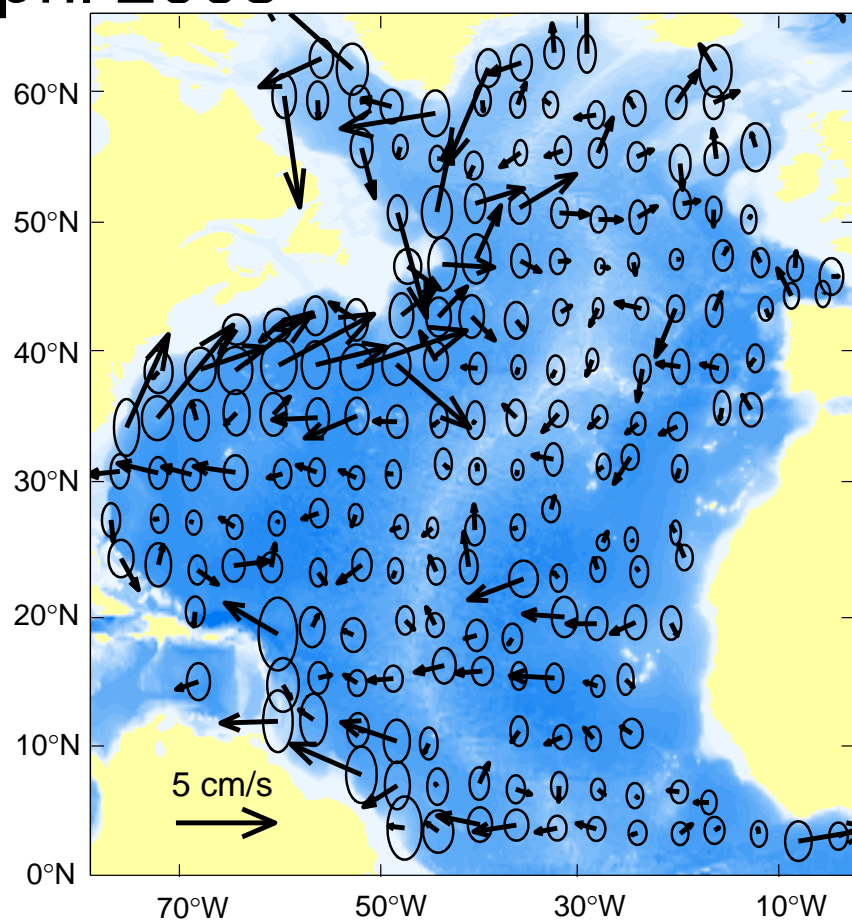
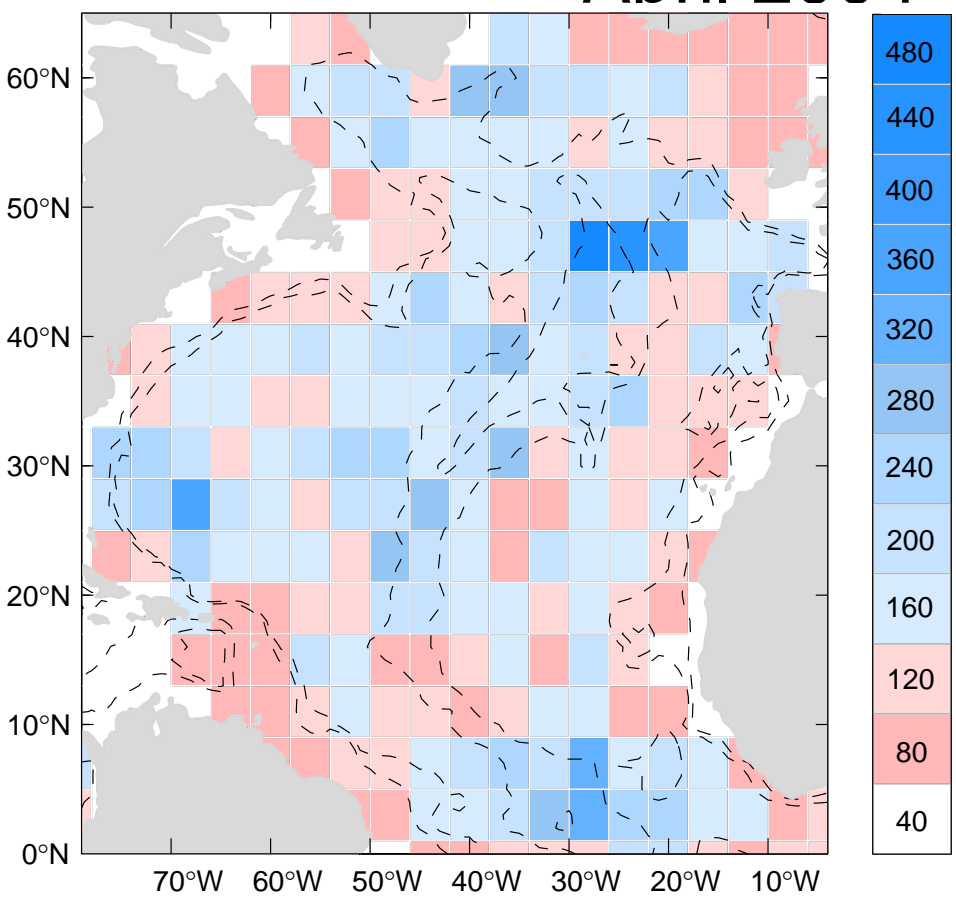


(b) Float positions where (T,S) were measured



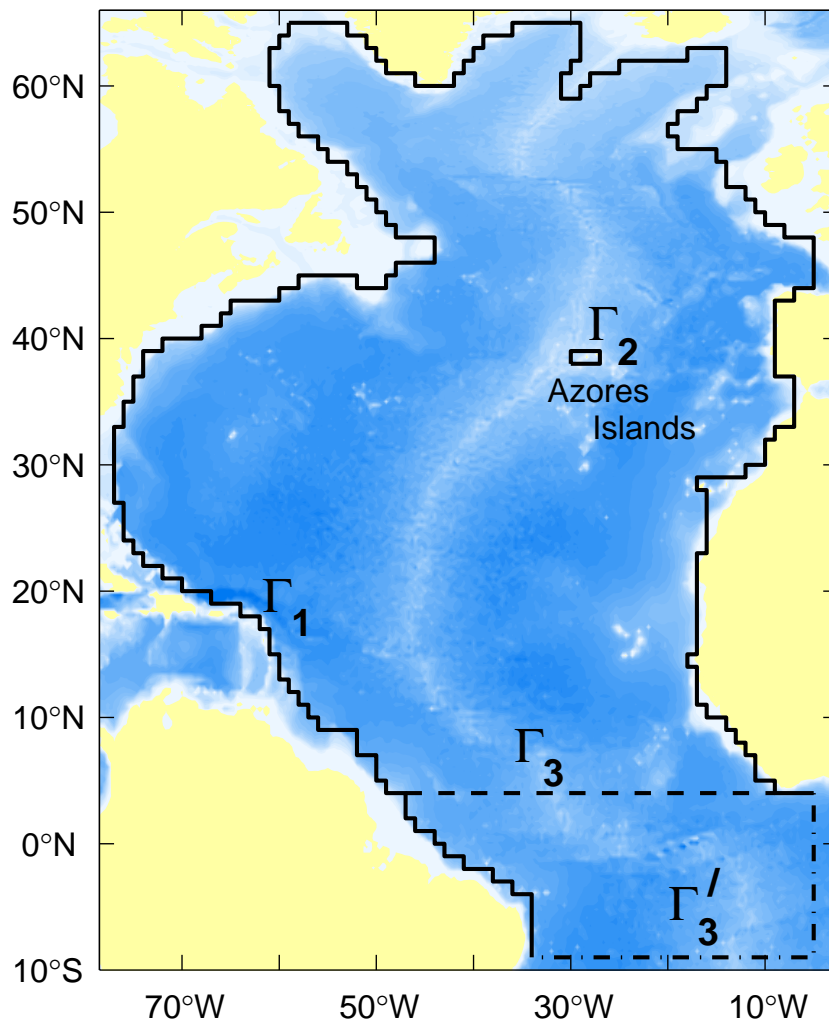
# Circulations at 1000 m estimated from the original ARGO float tracks (bin method)

April 2004 – April 2005

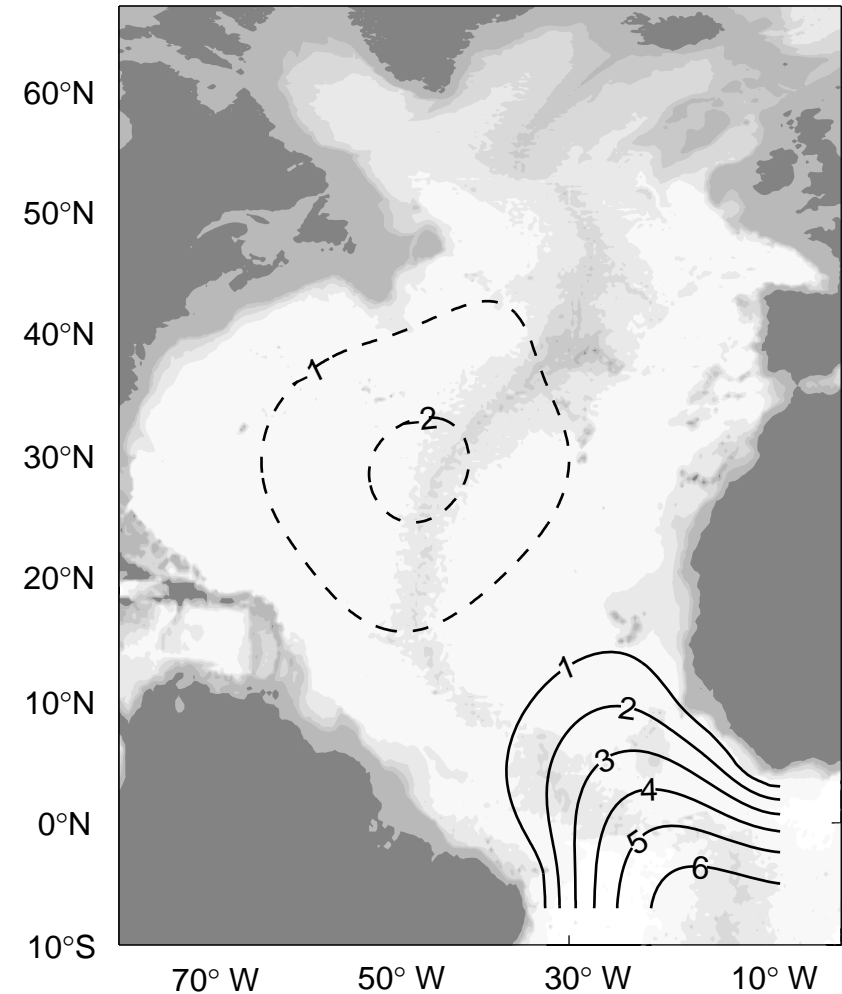
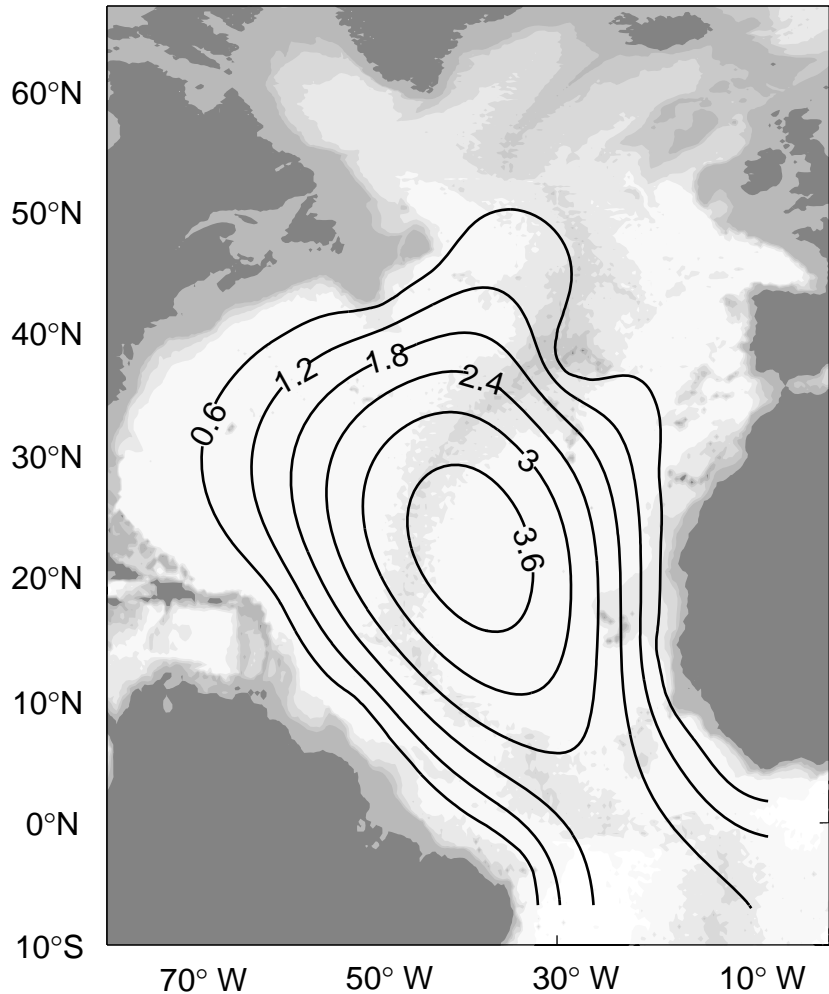


It is **difficult** to get physical insights and  
to use such noisy data into ocean numerical models.

# Boundary Configuration → Basis Functions for OSD



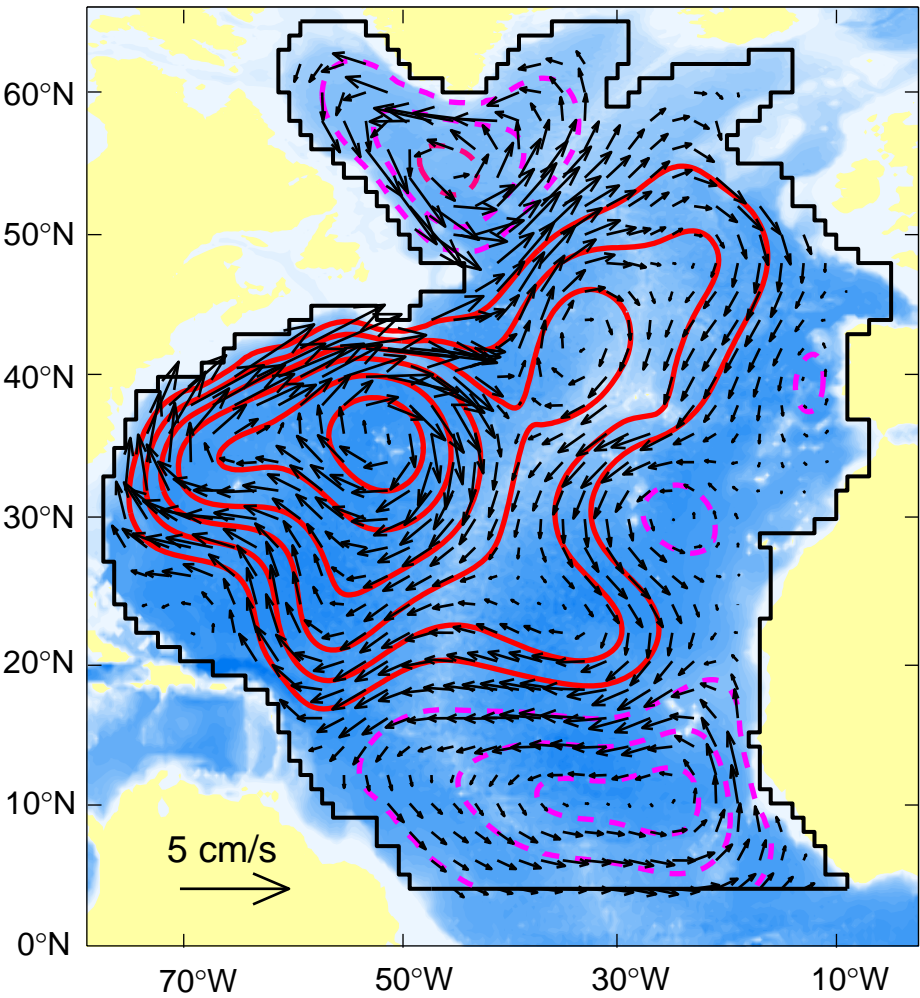
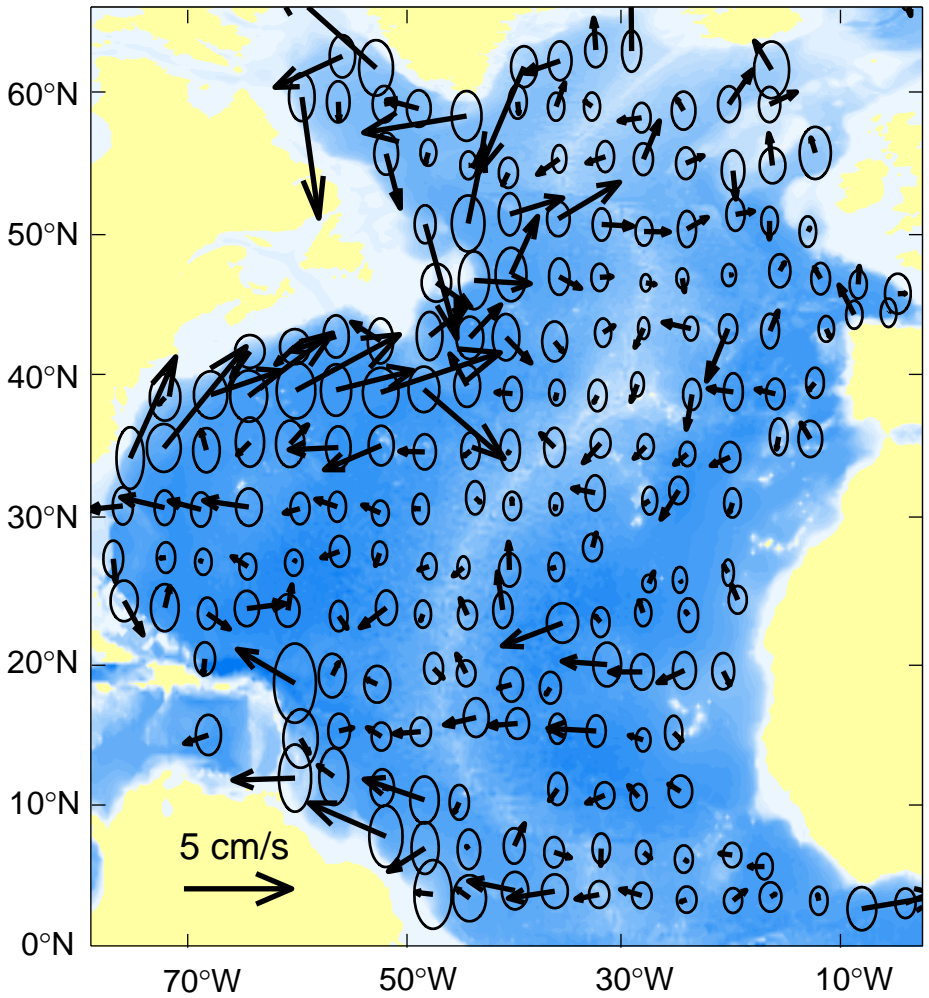
# Basis Functions for Streamfunction Mode-1 and Mode-2



# Circulations at 1000 m (March 04 to May 05)

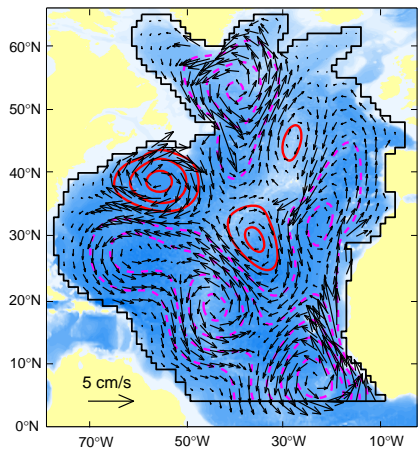
Bin Method

OSD

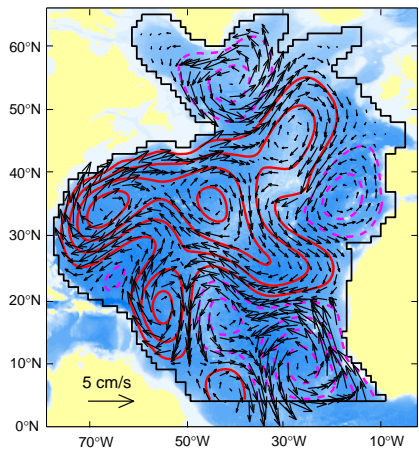


# Mid-Depth Circulations (1000 m)

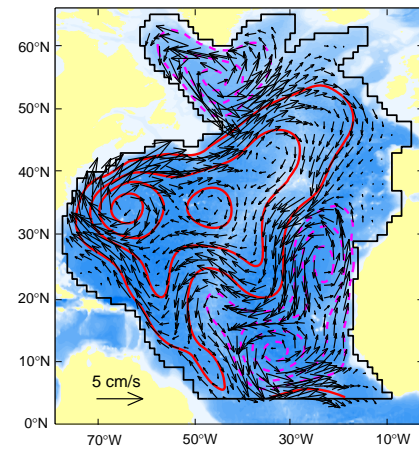
Mar-May 04



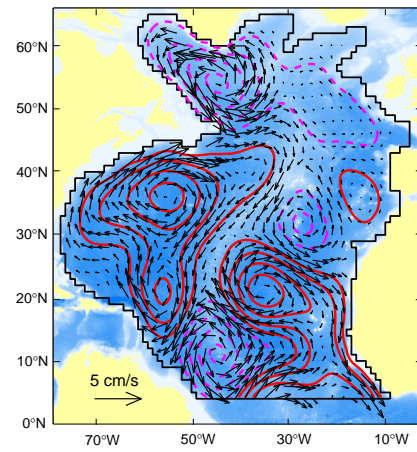
May – Jul 04



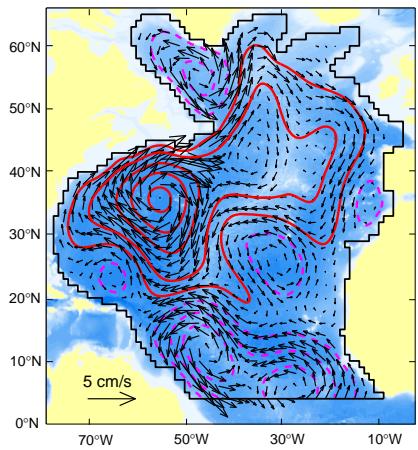
Jul-Sep 04



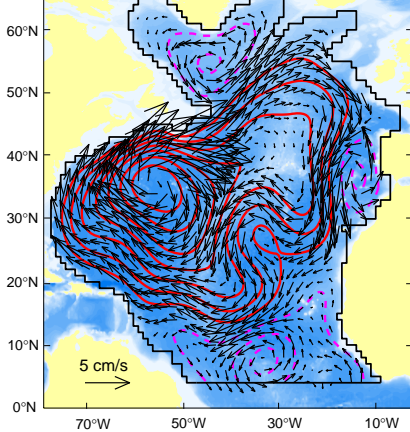
Sep – Nov 04



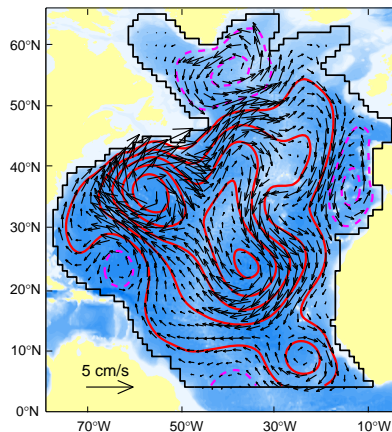
Nov 04 – Jan 05



Jan-Mar 05



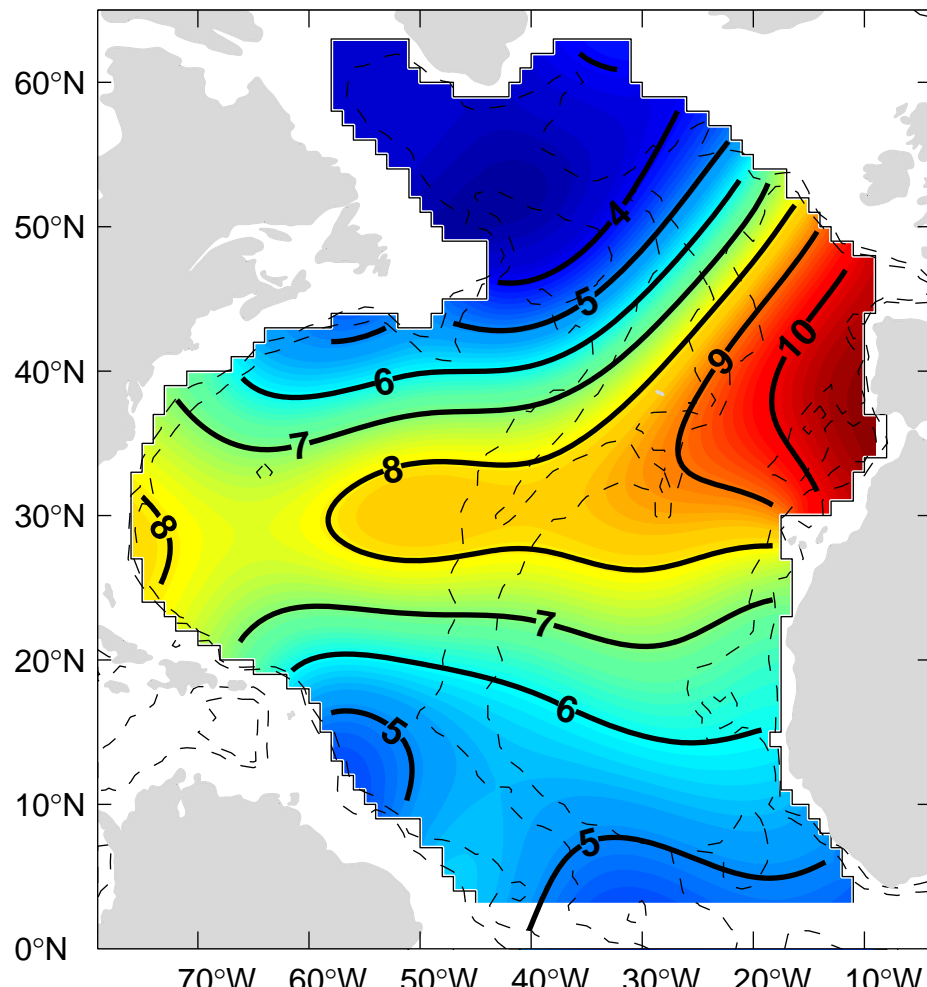
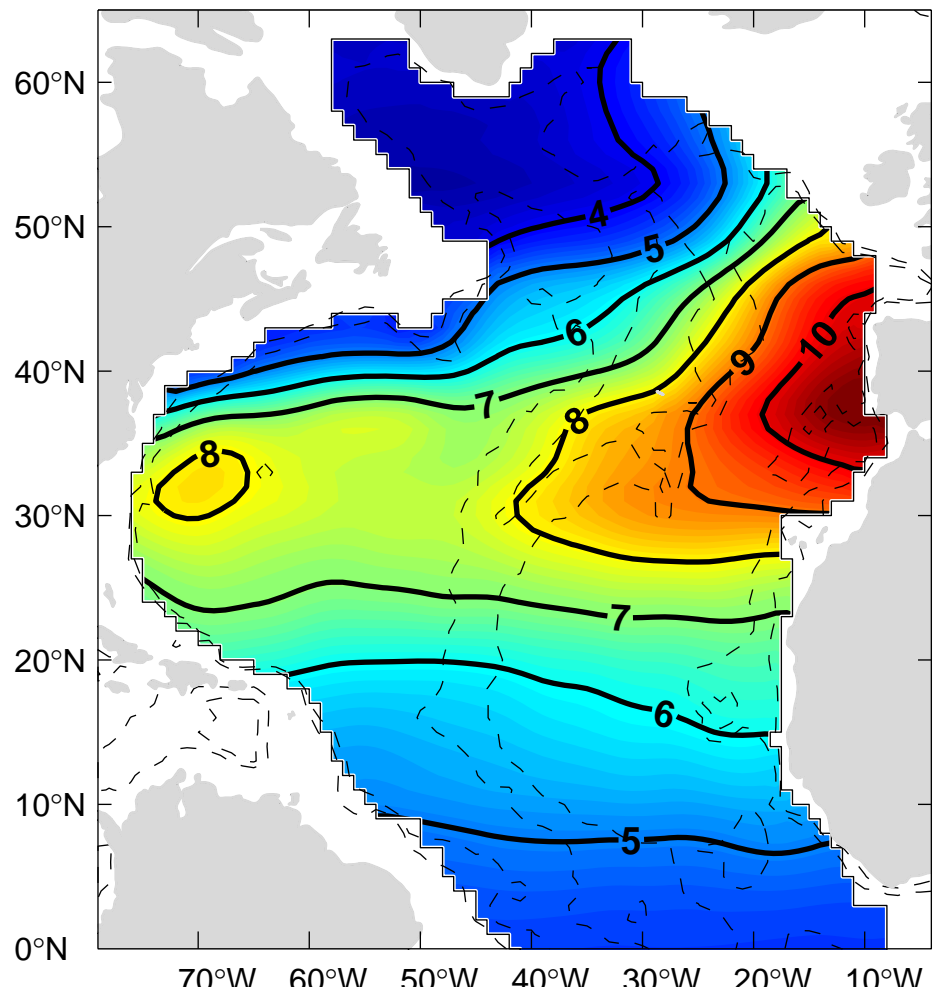
Mar – May 05



# Temperature at 950 m (March 04 to May 05)

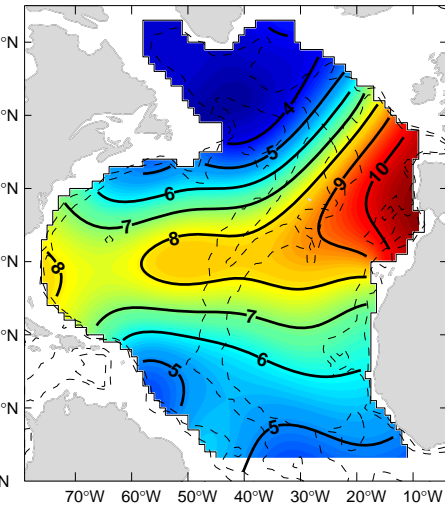
## NOAA/WOA

## OSD

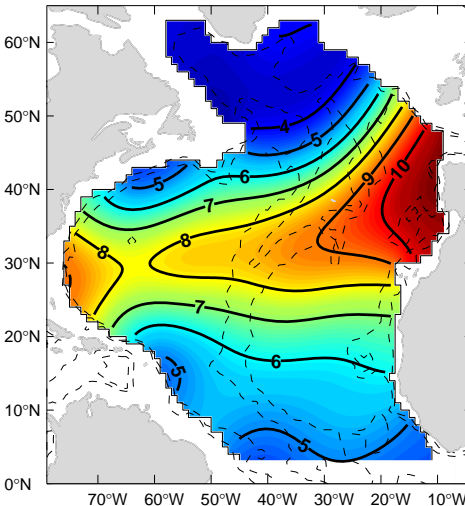


# Mid-Depth Temperature (950 m)

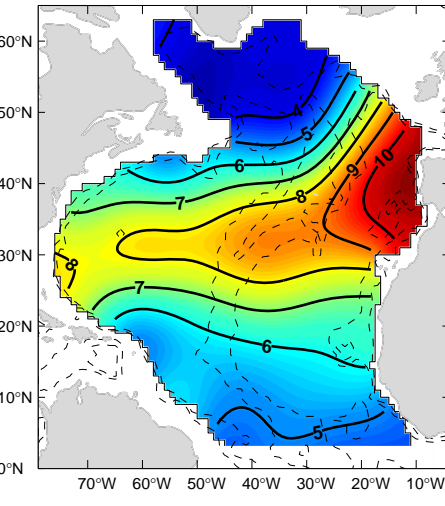
May 04



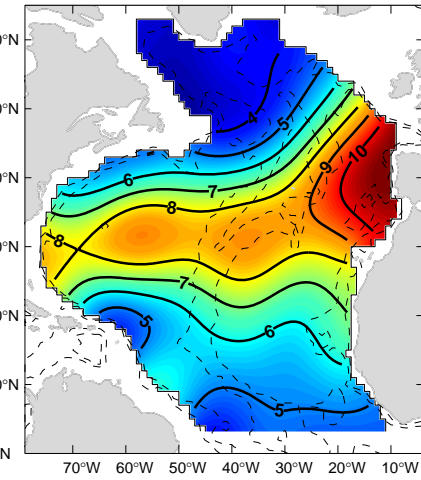
Jul 04



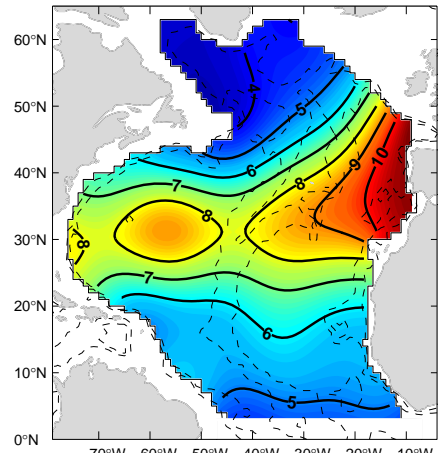
Sep 04



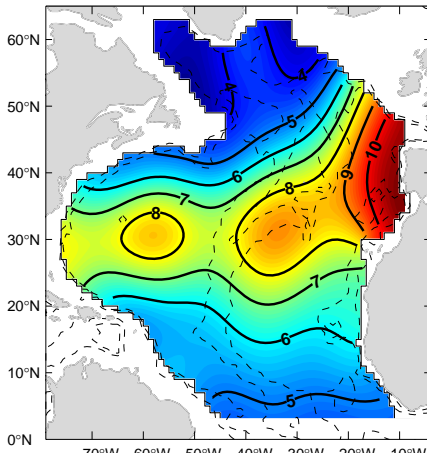
Nov 04



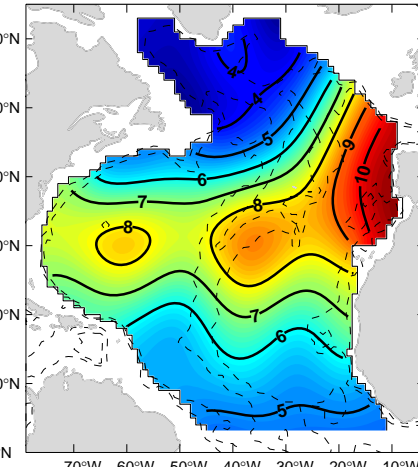
Jan 05



Mar 05



May 05



# Baroclinic Rossby Waves in Tropical North Atlantic

# Fourier Expansion → Temporal Annual and Semi-annual

$$\hat{\psi} \approx \bar{\psi}(\mathbf{x}_\perp) + \psi_1(\mathbf{x}_\perp, t) + \psi_2(\mathbf{x}_\perp, t),$$

$$\psi_1(\mathbf{x}_\perp, t) = \sum_{s=1}^2 A_{\omega_1, s} \cos(\omega_1 t + \theta_{\omega_1, s}) Z_s(\mathbf{x}_\perp) + \sum_{k=1}^{K_{opt}} B_{\omega_1, k} \cos(\omega_1 t + \vartheta_{\omega_1, k}) \Psi_k(\mathbf{x}_\perp),$$

$$\psi_2(\mathbf{x}_\perp, t) = \sum_{s=1}^2 A_{\omega_2, s} \cos(\omega_2 t + \theta_{\omega_2, s}) Z_s(\mathbf{x}_\perp) + \sum_{k=1}^{K_{opt}} B_{\omega_2, k} \cos(\omega_2 t + \vartheta_{\omega_2, k}) \Psi_k(\mathbf{x}_\perp),$$

$$T_0 = 12 \text{ months}; \quad \omega_1 = 2\pi/T_0 ; \quad \omega_2 = 4\pi/T_0$$

# Fourier Expansion → Temporal Annual and Semi-annual

$$\hat{T}(\mathbf{x}_\perp, z, t) \approx \bar{T}(\mathbf{x}_\perp, z) + T_1(\mathbf{x}_\perp, z, t) + T_2(\mathbf{x}_\perp, z, t),$$

$$T_1(\mathbf{x}_\perp, z, t) = \sum_{m=1}^{M_{opt}} C_{\omega_1, m}(z) \cos[\omega_1 t + \chi_{\omega_1, m}(z)] \Xi_m(\mathbf{x}_\perp, z),$$

$$T_2(\mathbf{x}_\perp, z, t) = \sum_{m=1}^{M_{opt}} C_{\omega_2, m}(z) \cos[\omega_2 t + \chi_{\omega_2, m}(z)] \Xi_m(\mathbf{x}_\perp, z),$$

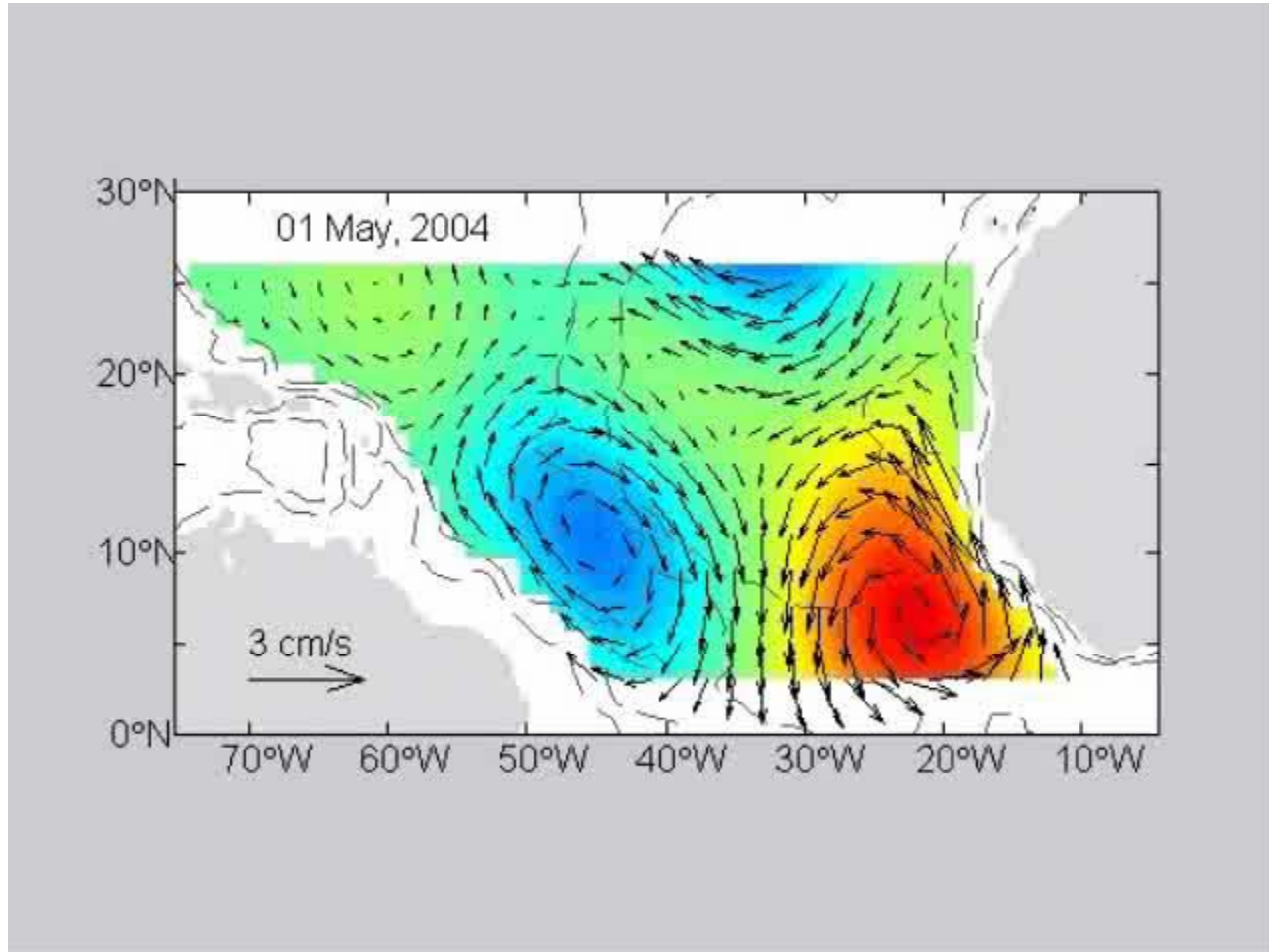
$$T_0 = 12 \text{ months}; \quad \omega_1 = 2\pi/T_0 ; \quad \omega_2 = 4\pi/T_0$$

# Optimization

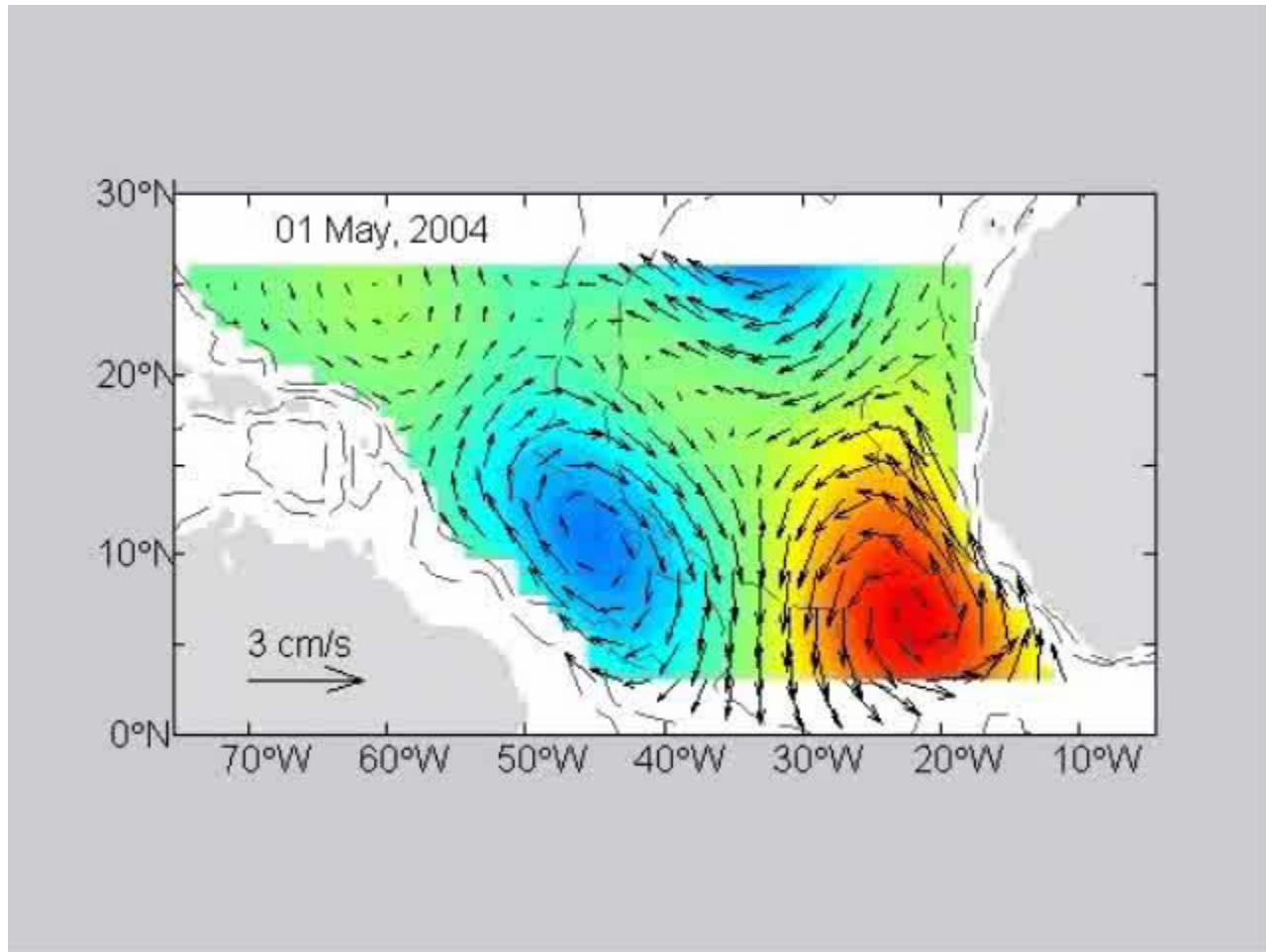
$$J_s = \int_{t_o}^{t_o + T_o} \left[ a_s(t) - \sum_{\omega=\omega_1, \omega_2} A_{\omega, s} \cos(\omega t + \theta_{\omega, s}) \right]^2 dt \rightarrow \min$$

$$I_k = \int_{t_o}^{t_o + T_o} \left[ b_k(t) - \sum_{\omega=\omega_1, \omega_2} B_{\omega, s} \cos(\omega t + \vartheta_{\omega, s}) \right]^2 dt \rightarrow \min$$

# Annual Component

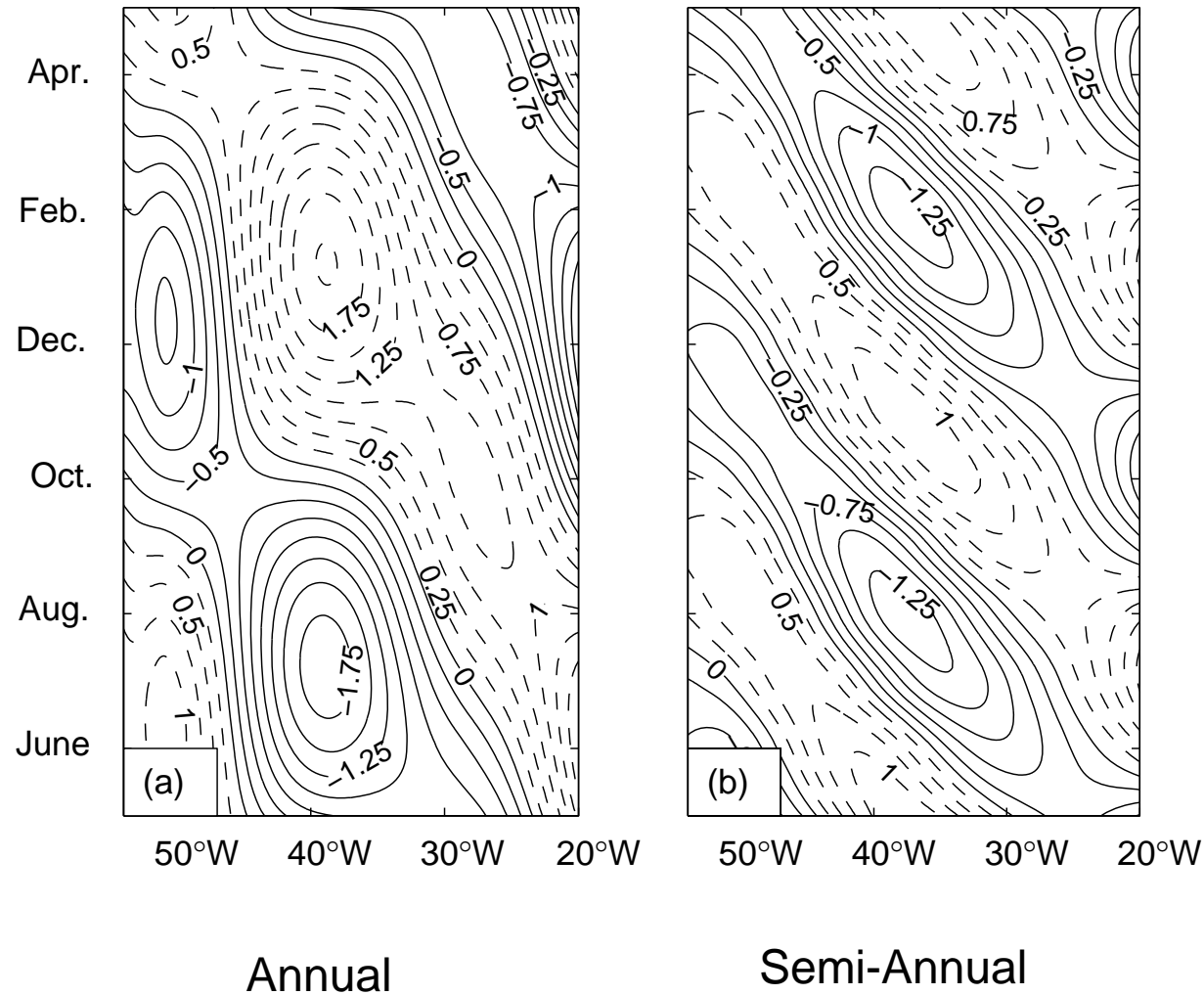


# Semi-annual Component

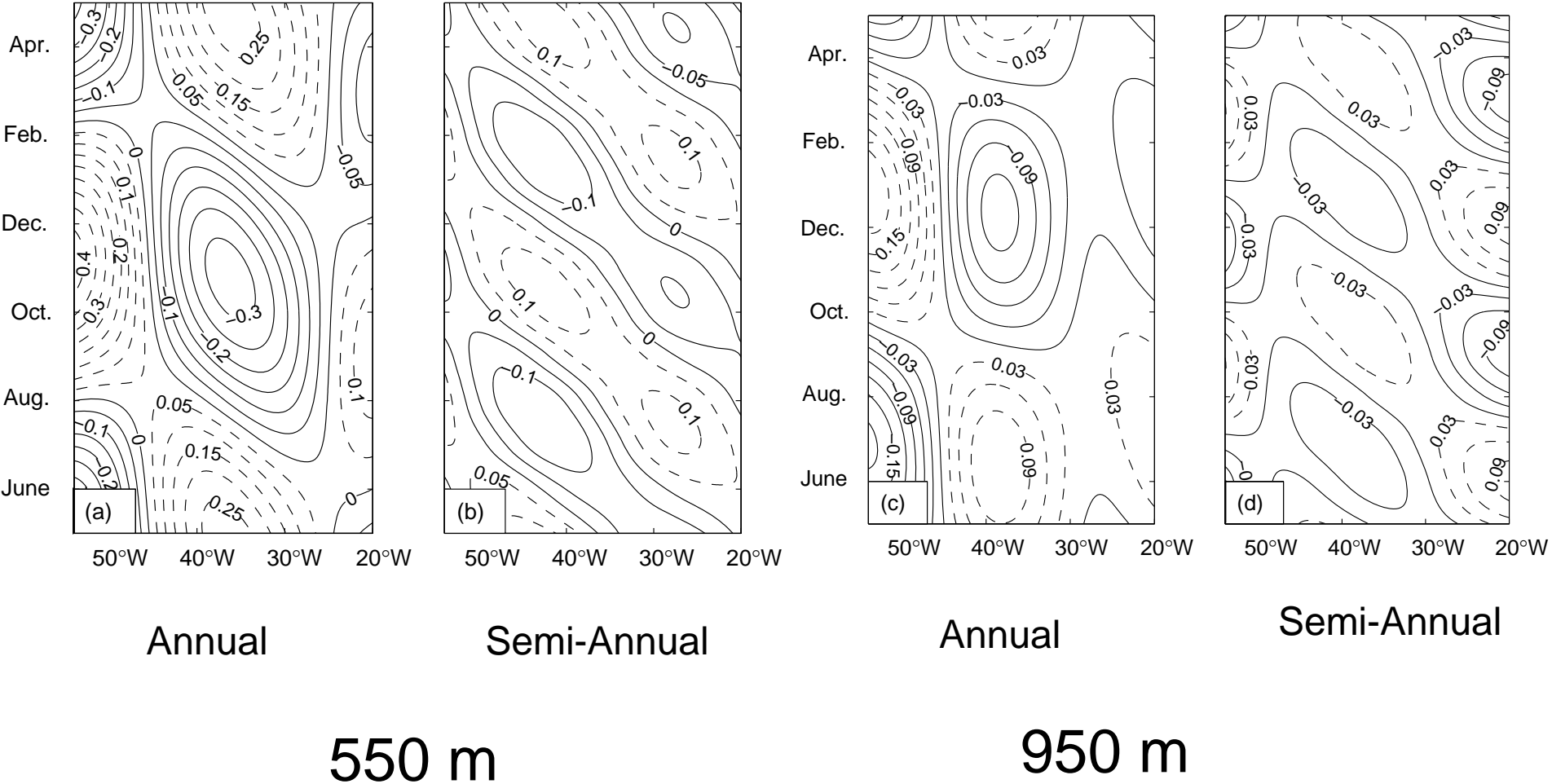


# Time –Longitude Diagrams of Meridional Velocity

## Along $11^{\circ}\text{N}$



# Time –Longitude Diagrams of temperature Along 11°N



# Characteristics of Annual Rossby Waves

	March, 04 – May, 05 float data			March, 04 – May, 06 float data		
Latitude	$c_p$ (cm/s)	$L_1$ (km)	$L_2$ (km)	$c_p$ (cm/s)	$L_1$ (km)	$L_2$ (km)
5°N	12	1200	1100	12	1300	900
8°N	16	2500	1400	12	2100	1100
11°N	14	2200	1400	11	1900	1100
13°N	11	2100	1500	10	2300	1500

Western  
Basin

Eastern  
Basin

Western  
Basin

Eastern  
Basin

# Results

- The annual and semi-annual unstable standing Rossby waves are detected in both the western and eastern sub-basins.
- The wind-driven Ekman pumping seems to be responsible for the wave generation in both the sub-basins.

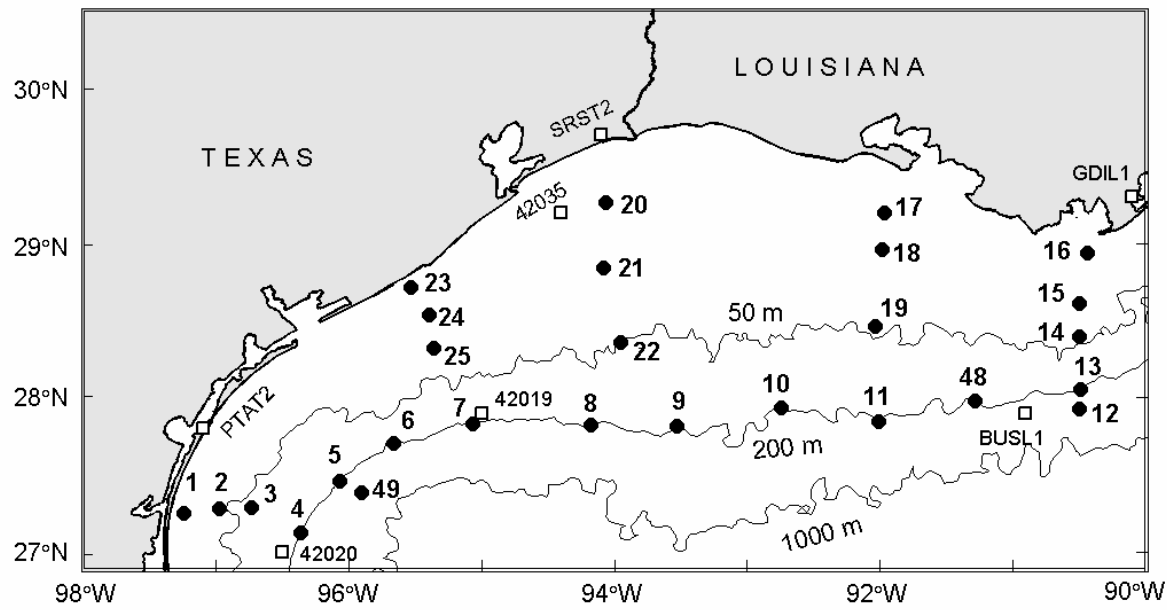
# Example-2

## OSD for Analyzing Combined Current Meter and Surface Drifting Buoy Data

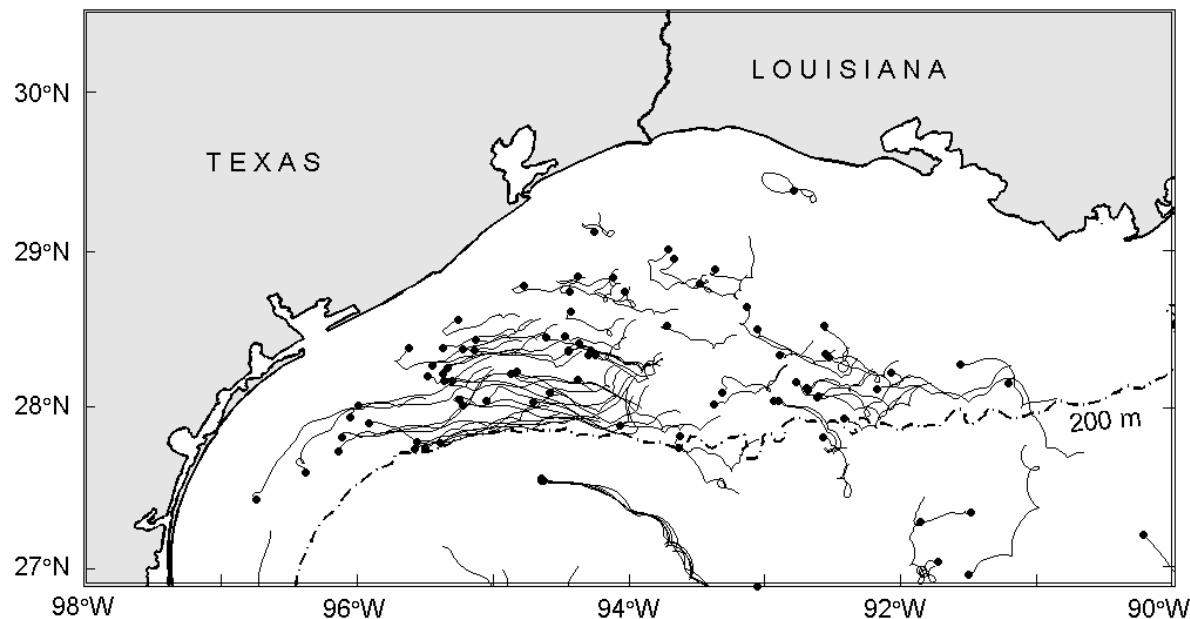
# Ocean Velocity Observation

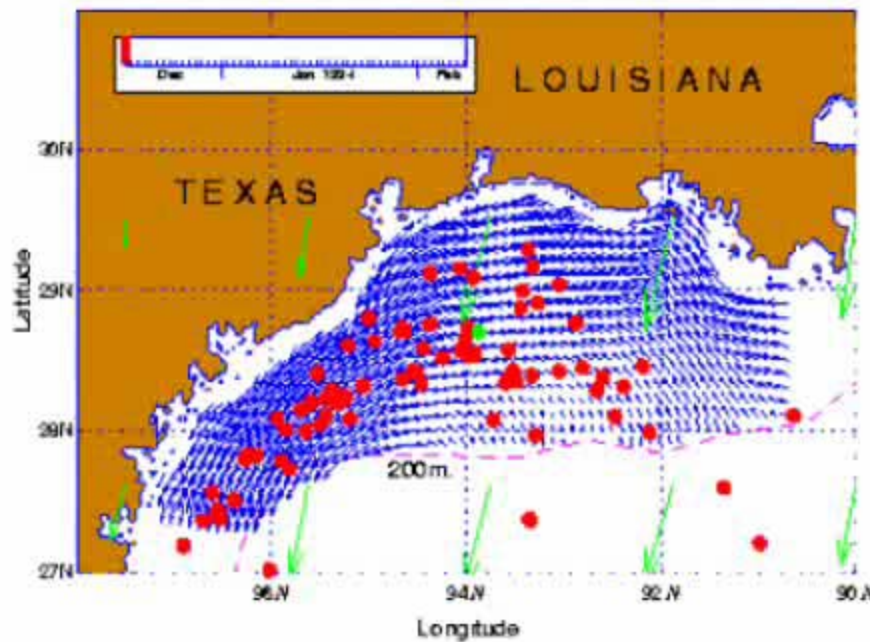
- 31 near-surface (10-14 m) current meter moorings during LATEX from April 1992 to November 1994
- Drifting buoys deployed at the first segment of the Surface Current and Lagrangian-drift Program (SCULP-I) from October 1993 to July 1994.

# Moorings

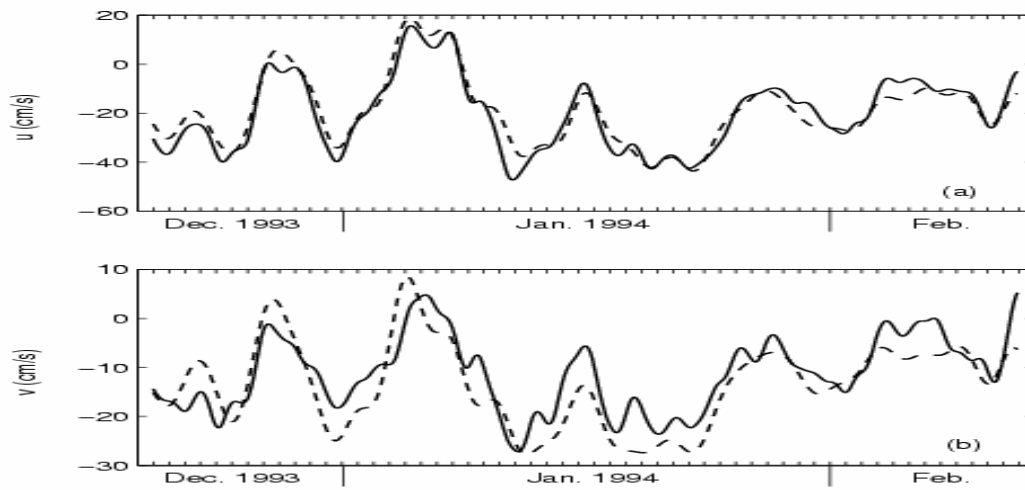


# LTCS current reversal detected from SCULP-I drift trajectories.





# Reconstructed and observed circulations at Station-24.



# Probability of TLCS Current Reversal for Given Period (T)

- $n_0$  ~0-current reversal
- $n_1$ ~ 1-current reversal
- $n_2$ ~ 2-current reversals
- m ~ all realizations

$$P_0(T) = \frac{n_0}{m}, P_1(T) = \frac{n_1}{m}, P_2(T) = \frac{n_2}{m},$$

# Fitting the Poisson Distribution

$$P_k(T) = \frac{1}{k!} (\mu T)^k \exp(-\mu T)$$

$$k=0, 1, 2$$

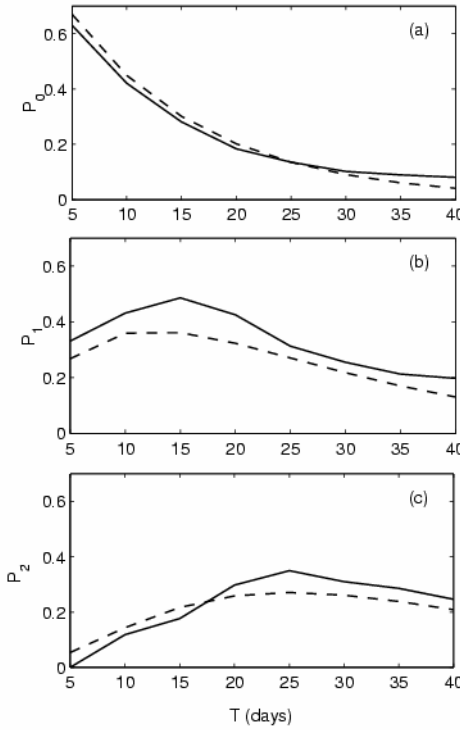
$\mu$  is the mean number of reversal for a single time interval

$$\mu \sim 0.08$$

# Dependence of $P_0$ , $P_1$ , $P_2$ on $T$

For observational periods larger than 20 days, the probability for no current reversal is less than 0.2.

For 15 day observational period, the probability for 1-reversal reaches 0.5



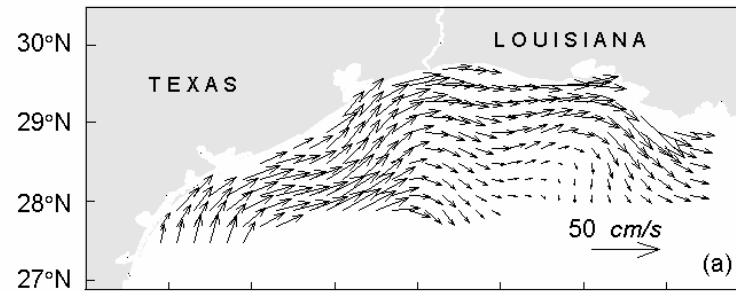
Data – Solid Curve  
Poison Distribution Fitting –  
Dashed Curve

# Time Interval between Successive Current Reversals (not a Rare Event)

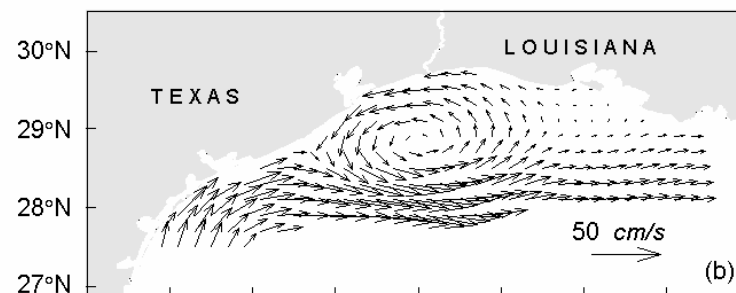
$$p(\tau) = \mu \exp(-\mu\tau)$$

# LTCs current reversal detected from the reconstructed velocity data

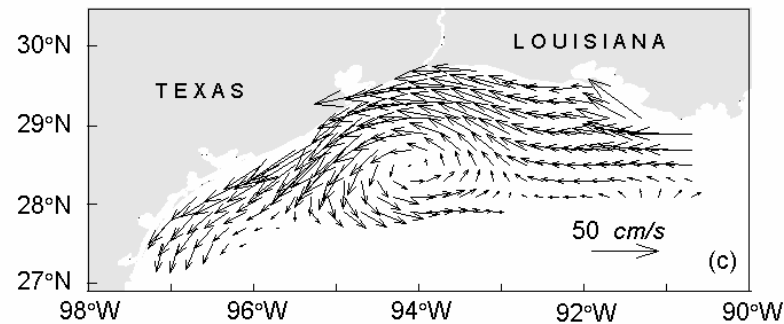
December 30, 1993



January 3, 1994



January 6, 1994



# EOF Analysis of the Reconstructed Velocity Filed

EOF	Variance (%)		
	01/21/93-05/21/93	12/19/93-04/17/94	10/05/94-11/29/94
1	80.2	77.1	74.4
2	10.1	9.5	9.3
3	3.9	5.6	6.9
4	1.4	3.3	4.6
5	1.1	1.4	2.3
6	0.7	1.1	0.8

# Mean and First EOF Mode

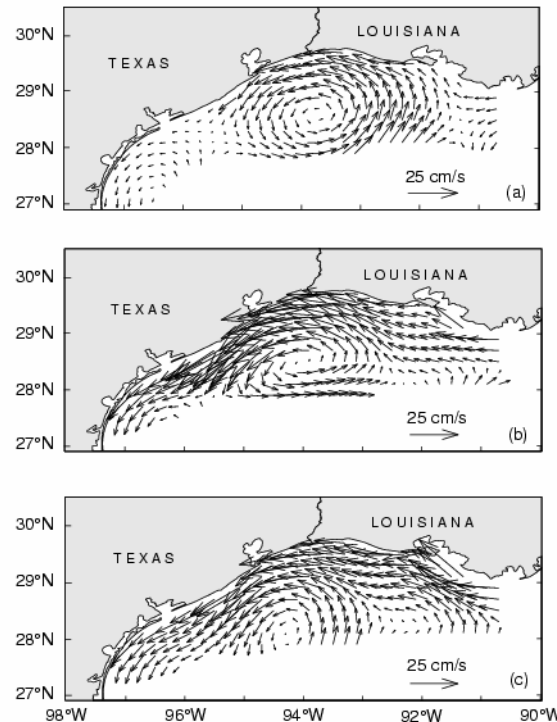
$$\tilde{\mathbf{u}}(x, y, t) = \bar{\mathbf{u}}(x, y) + A_1(t)\mathbf{u}_1(x, y),$$

# Mean Circulation

1. First Period  
(01/21-05/21/93)

2. Second Period  
12/19/93-04/17/94)

3. Third Period  
(10/05-11/29/94)

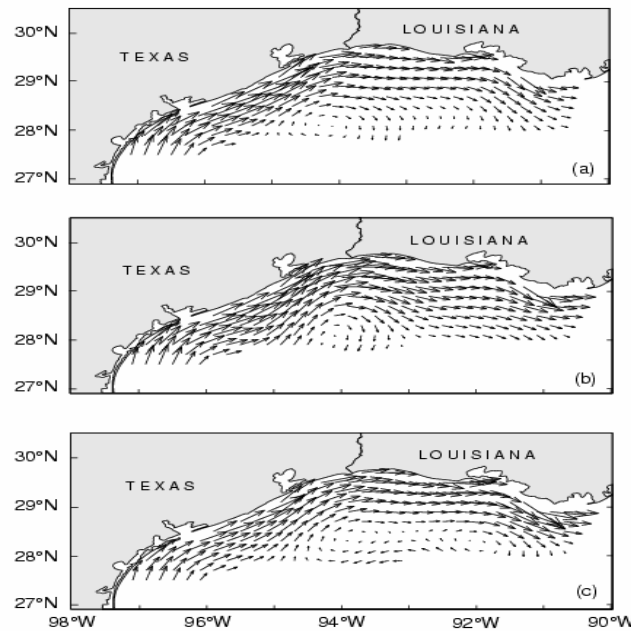


# EOF1

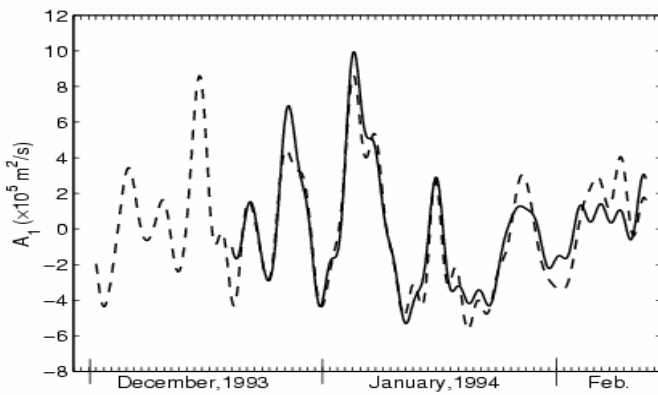
1. First Period  
(01/21-05/21/93)

2. Second Period  
12/19/93-04/17/94)

3. Third Period  
(10/05-11/29/94)



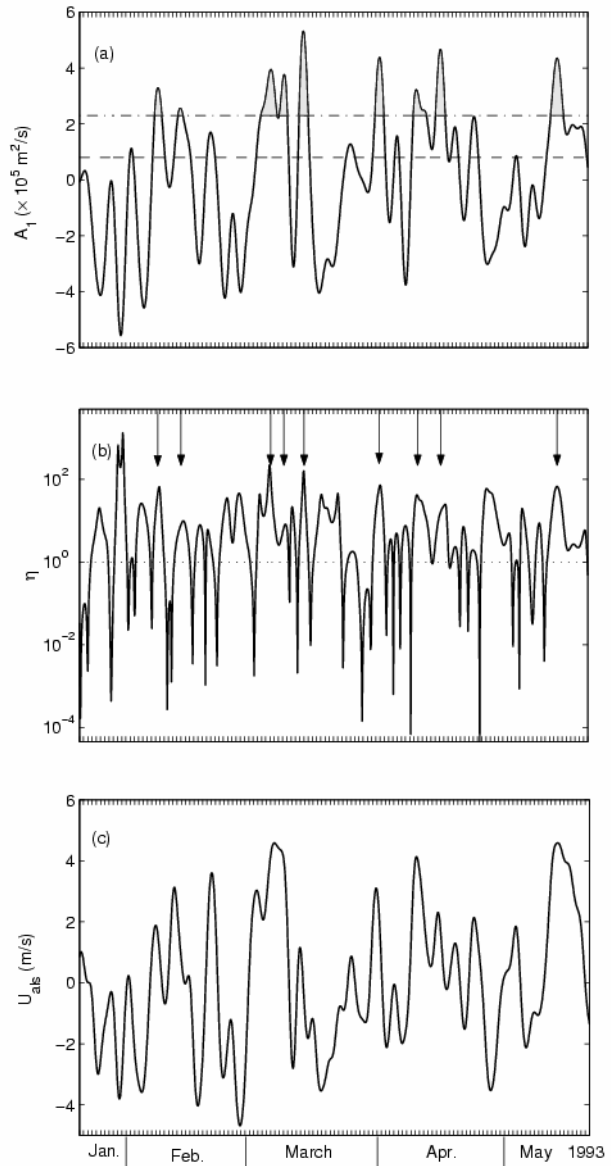
- Calculated  $A_1(t)$   
Using Current Meter  
Mooring (solid)  
and SCULP-1  
Drifters (dashed)



- 8 total reversals observed

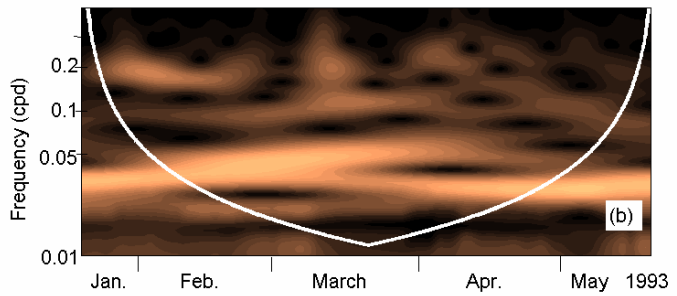
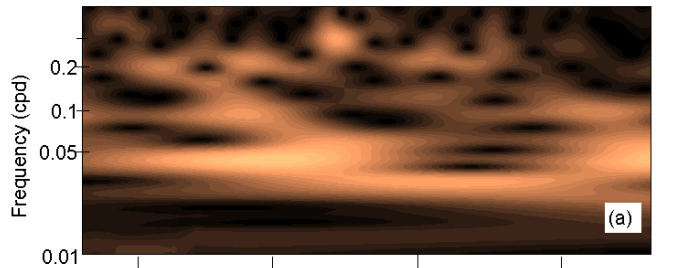
$$\eta = A_1^2 / \sum_{n=2}^6 A_n^2$$

- $U_{als} \sim$  alongshore wind



# Morlet Wave

- $A_1(t)$

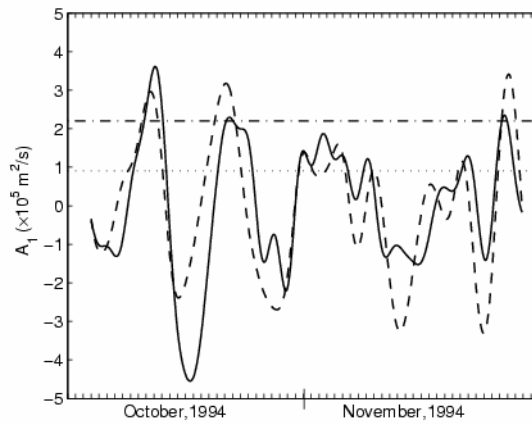


$$\Phi(t) = \pi^{-4} \exp(imt - t^2/2), \quad m = 6$$

# Surface Wind Data

- 7 buoys of the National Data Buoy Center (NDBC) and industry (C-MAN) around LATEX area

- Regression between
- $A_1(t)$  and Surface Winds
- Solid Curve (reconstructed)
- Dashed Curve (predicted using winds)



$$A_1(t) = \alpha[U(t) - \bar{U}] + \beta[V(t) - \bar{V}] + \gamma$$

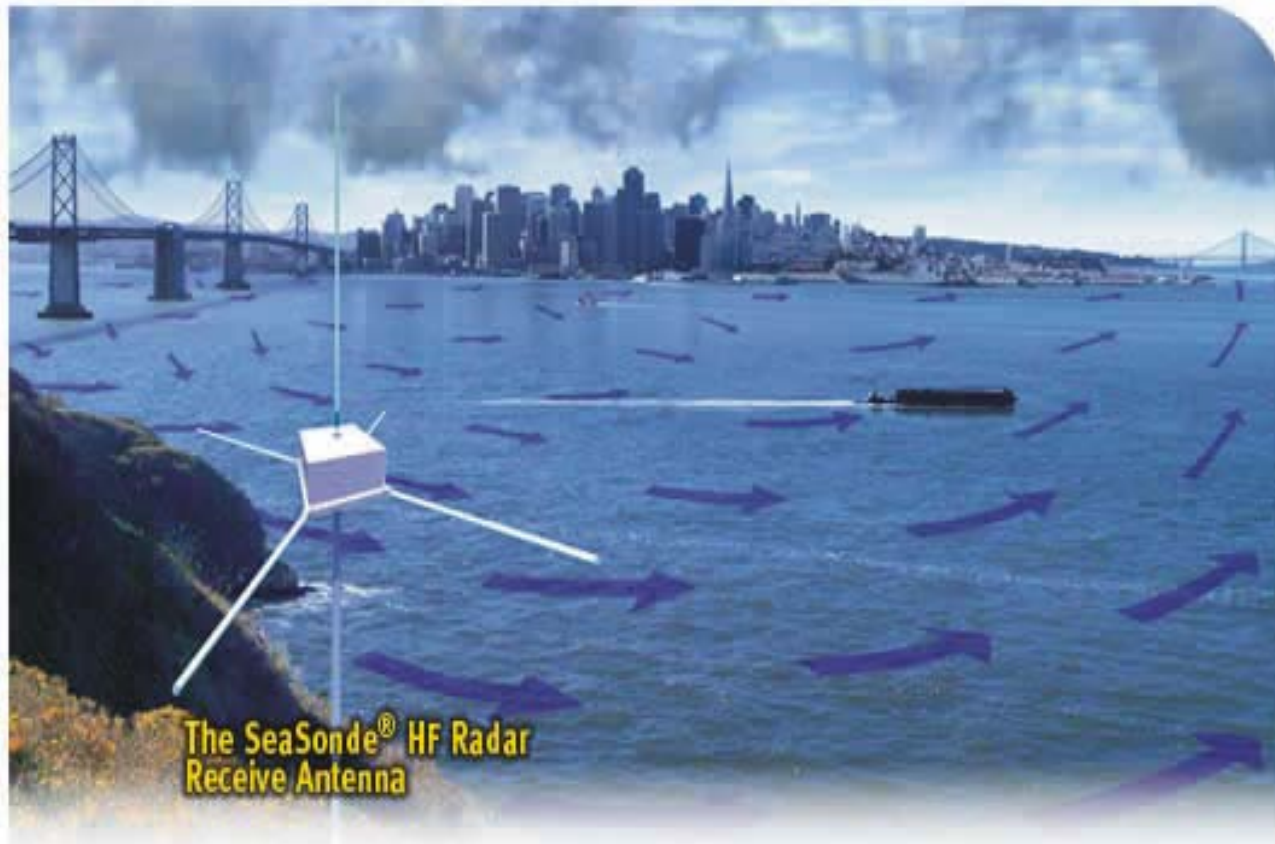
# Results

- Alongshore wind forcing is the major factor causing the synoptic current reversal.
- Other factors, such as the Mississippi-Atchafalaya River discharge and offshore eddies of Loop Current origin, may affect the reversal threshold, but can not cause the synoptic current reversal.

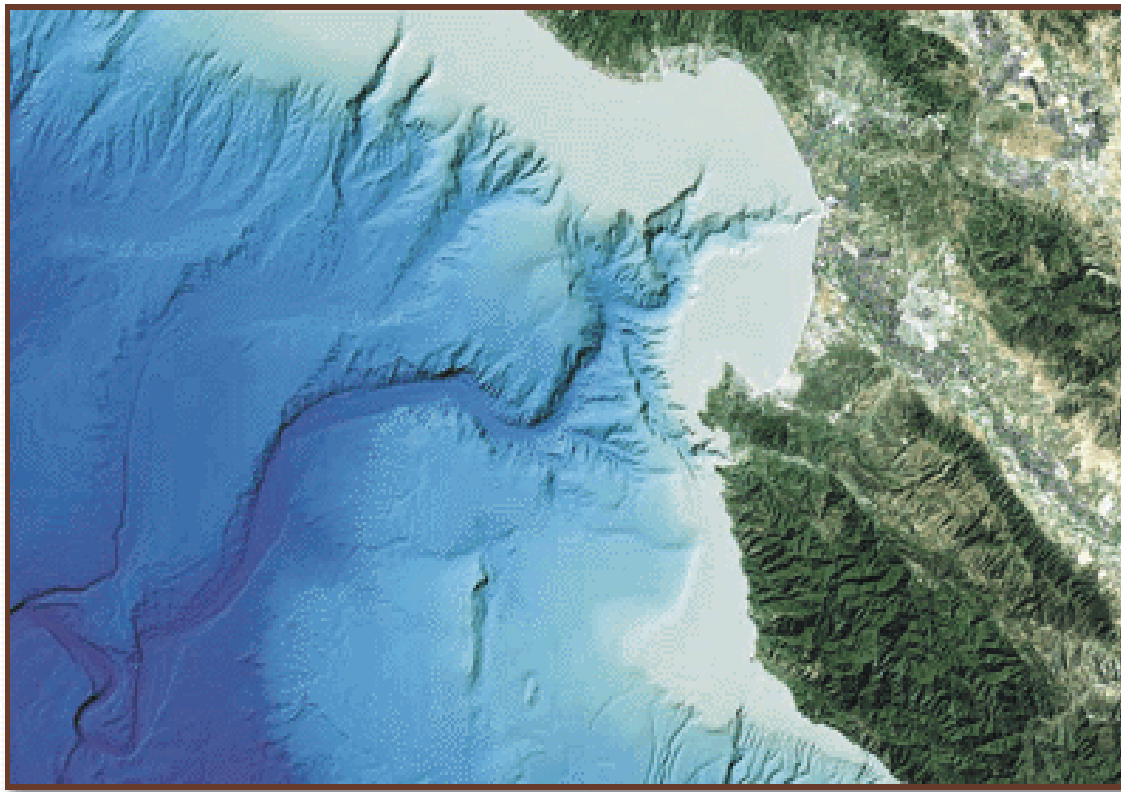
# Part-3

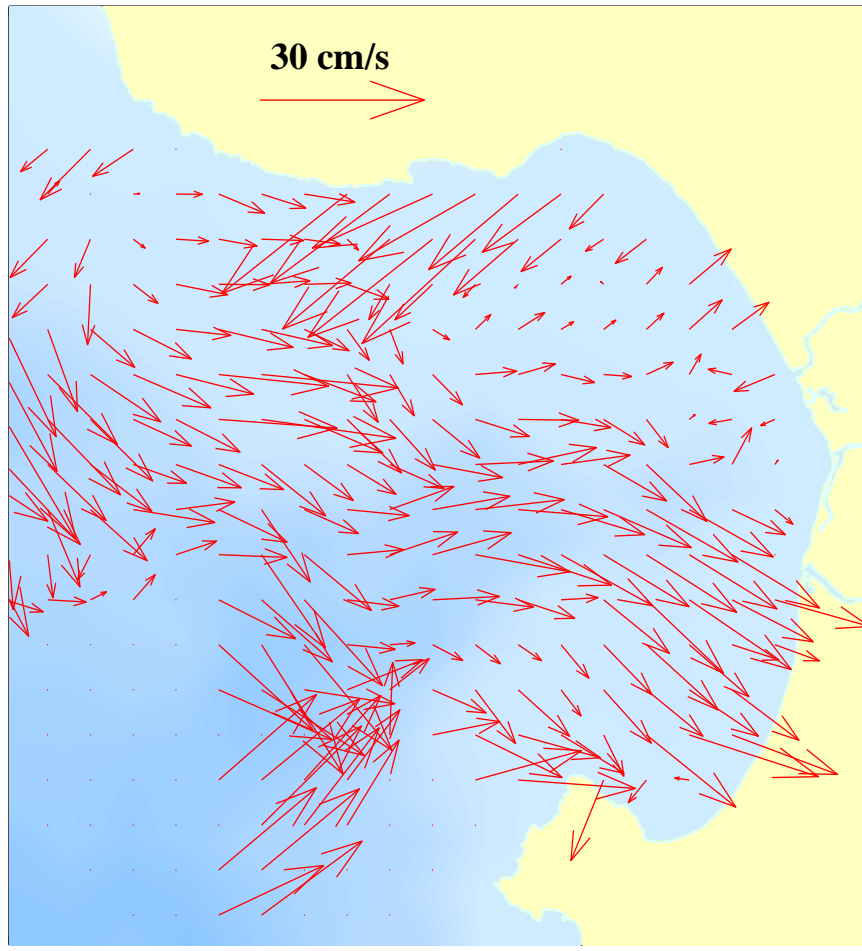
# OSD for Analyzing CODAR Data

# CODAR

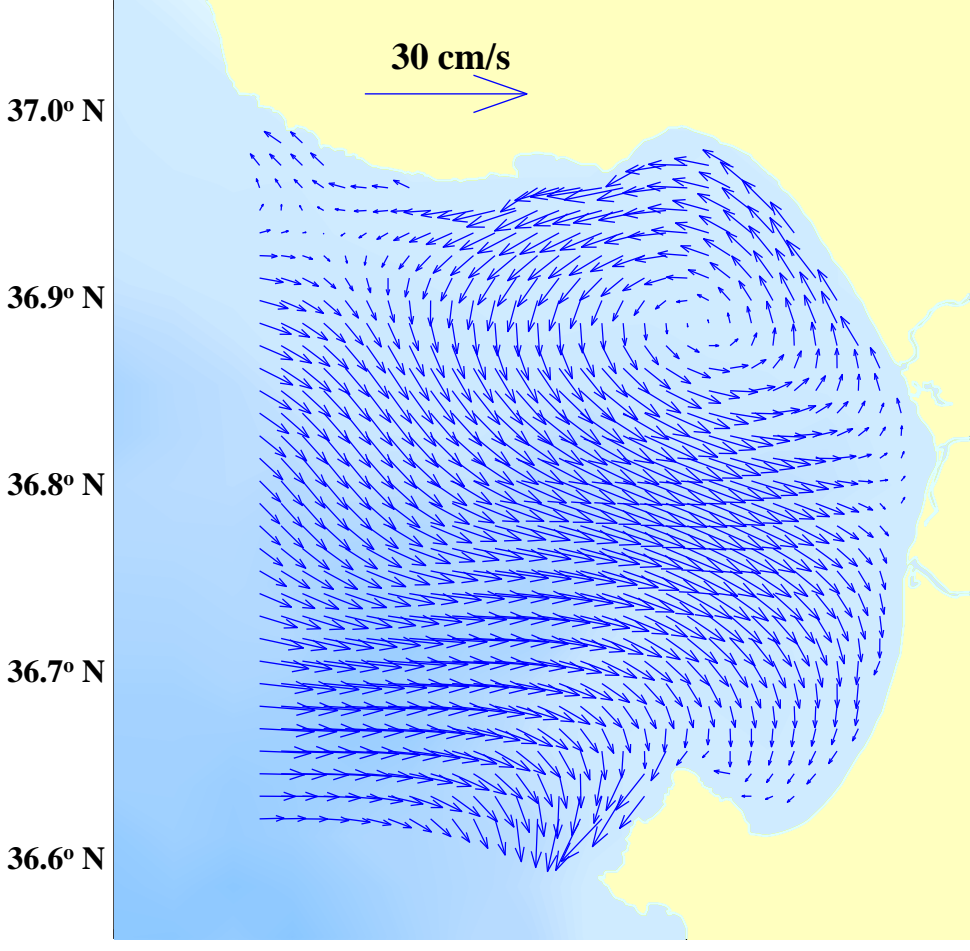


# Monterey Bay





122.2° W    122.1° W    122.0° W    121.9° W    121.8° W



122.2° W    122.1° W    122.0° W    121.9° W    121.8° W

Place for comments: left - radar derived currents for 17:00 UT December 1, 1999

right – reconstructed velocity field.

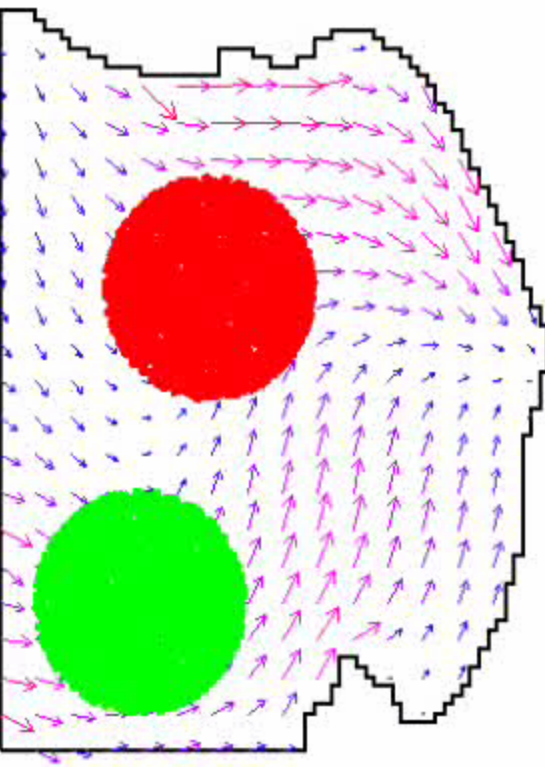
cm/sec

CODAR Velocity  
0000 UT, 3 June 1999

35  
30  
25  
20  
15  
10  
5  
0

→ 25 cm s<sup>-1</sup>

10 Mode Nowcast



# Conclusions

- OSD is a useful tool for processing real-time velocity data with short duration and limited-area sampling especially the ARGO data.
- OSD has wide application in ocean data assimilation.